



**HAL**  
open science

# The spring mesozooplankton variability and its relationship with hydrobiological structure over year-to-year changes (2003–2013) in the southern Bay of Biscay (Northeast Atlantic)

Aurélie Dessier, Paco Bustamante, Tiphaine Chauvelon, Martin Huret, Marc Pagano, Elise Marquis, Frederic Rousseaux, Cécilia Pignon-Mussaud, Françoise Mornet, Christine Dupuy

## ► To cite this version:

Aurélie Dessier, Paco Bustamante, Tiphaine Chauvelon, Martin Huret, Marc Pagano, et al.. The spring mesozooplankton variability and its relationship with hydrobiological structure over year-to-year changes (2003–2013) in the southern Bay of Biscay (Northeast Atlantic). *Progress in Oceanography*, 2018, 166, pp.76-87. 10.1016/j.pocean.2018.04.011 . hal-01926540

**HAL Id: hal-01926540**

**<https://hal.science/hal-01926540>**

Submitted on 19 Nov 2018

**HAL** is a multi-disciplinary open access archive for the deposit and dissemination of scientific research documents, whether they are published or not. The documents may come from teaching and research institutions in France or abroad, or from public or private research centers.

L'archive ouverte pluridisciplinaire **HAL**, est destinée au dépôt et à la diffusion de documents scientifiques de niveau recherche, publiés ou non, émanant des établissements d'enseignement et de recherche français ou étrangers, des laboratoires publics ou privés.

1 **The spring mesozooplankton variability and its relationship with hydrobiological**  
2 **structure over year-to-year changes (2003–2013) in the southern Bay of Biscay**  
3 **(Northeast Atlantic)**

4  
5 Aurélie Dessier<sup>1</sup>, Paco Bustamante<sup>1</sup>, Tiphaine Chouvelon<sup>2</sup>, Martin Huret<sup>3</sup>, Marc Pagano<sup>4</sup>,  
6 Elise Marquis<sup>5</sup>, Frédéric Rousseaux<sup>1</sup>, Cécilia Pignon-Mussaud<sup>1</sup>, Françoise Mornet<sup>6</sup>, Martine  
7 Bréret<sup>1</sup>, and Christine Dupuy<sup>1\*</sup>

8  
9 <sup>1</sup>Littoral Environnement et Sociétés (LIENSs), UMR 7266, CNRS-Université de La Rochelle,  
10 2 rue Olympe de Gouges, 17042 La Rochelle Cedex 01, France

11 <sup>2</sup>IFREMER, Unité Biogéochimie et Écotoxicologie (BE), Laboratoire de Biogéochimie des  
12 Contaminants Métalliques (LBCM), Rue de l'Île d'Yeu, F-44311 Nantes 03, France

13 <sup>3</sup>IFREMER, Unité Sciences et Technologies Halieutiques (STH), Laboratoire de Biologie  
14 Halieutique (LBH), Centre Bretagne, F-70 29280 Plouzané, France

15 <sup>4</sup>Institut Méditerranéen d'Océanologie (M.I.O.), UM 110, Aix-Marseille Université,  
16 CNRS/IRD, Campus de Luminy, Marseille 13288, France

17 <sup>5</sup>URS Qatar LLC, 22108, Bin Jaham Al Kuwari Bldg., Al Saad St., Doha, Qatar

18 <sup>6</sup>IFREMER, Unité Halieutique Gascogne Sud (HGS), Station de La Rochelle, Place Gaby  
19 Coll, F-17087 L'Houmeau, France

20

21 \*Corresponding author: Christine Dupuy

22 Email address: christine.dupuy@univ-lr.fr

23 Tel: +33 (0) 5 46 45 72 18

24 **Abstract**

25         Mesozooplankton can be considered the most important secondary producers in  
26 marine food webs because they hold an intermediate position between the phytoplankton  
27 assemblage and the upper trophic levels. They also are a robust indicator of climatic and  
28 hydrological conditions. We conducted an analysis of the interannual variability of the spring  
29 mesozooplankton assemblage, as sampled by the PELGAS fisheries survey in the southern  
30 part of the Bay of Biscay (Northeast Atlantic Ocean) between 2003 and 2013. We examined  
31 hydrology and trophic drivers to explain the variability. Our results revealed that the  
32 subsurface temperature, the subsurface salinity, the biomasses of subsurface pico-, nano-, and  
33 microphytoplankton, and the copepod assemblage exhibited a recurrent spatial pattern that  
34 was driven mainly by freshwater and nutrient inputs from the main rivers. The  
35 mesozooplankton assemblage was dominated by copepods (82%), composed of coastal,  
36 neritic, and oceanic copepod genera that paralleled the various hydrological fronts converging  
37 in the southern Bay of Biscay. The copepod community displayed high temporal-variability;  
38 there were three periods of abundant adult copepods throughout the southern Bay of Biscay.  
39 The copepod community was structured primarily around the drive for resource control,  
40 especially by the microphytoplankton biomass (24.3% of the total variability), and to a lesser  
41 extent by hydrological features (13.7% of the total variability).

## 42 **Introduction**

43 Mesozooplankton (200–2,000  $\mu\text{m}$ ) play a pivotal role in marine ecosystems by transferring  
44 energy from primary producers to the upper trophic levels. They are very sensitive to  
45 hydroclimatic features, so climate-mediated changes in zooplankton abundance and  
46 composition may affect upper trophic levels and fisheries (Beaugrand, 2003). Zooplankton  
47 monitoring therefore represents a powerful tool to detect, understand, and anticipate how  
48 global changes induce modifications in pelagic ecosystems (Beaugrand et al., 2003;  
49 Beaugrand, 2004; Perry et al., 2004; Richardson, 2008; Hinder et al., 2014). Although  
50 extensive and long-term zooplankton surveys have been undertaken (ICES Working Group on  
51 Zooplankton Ecology Zooplankton Status Report: <http://wgze.net/zooplankton-status-report>;  
52 O'Brien et al., 2013), they still are in relatively short supply compared to fish time-series from  
53 commercial catches (Batchelder et al., 2012).

54 In this study, we investigated the assemblage structure of mesozooplankton (at the  
55 level of the species, genus, or family) in the Bay of Biscay, an important Northeast Atlantic  
56 fisheries area and a relatively stable ecosystem that primarily is structured around bottom-up  
57 forces (e.g., Lassalle et al., 2014). Our investigation covers a large spatio-temporal scale: from  
58 the Spanish coast at 46°N to the French coast at 3°35'W, from the spring of 2003 through the  
59 spring of 2013. Previous mesozooplankton studies in the Bay of Biscay have been conducted  
60 in the spring as well because it is the key period for plankton blooms and the reproductive  
61 period for anchovies and sardines (Huret et al., this issue). Although some of these studies  
62 considered large spatial and/or temporal scales, they had more limited scopes; some relied on  
63 the LOPC (Laser Optical Plankton Counter) technique and were limited to size-structure  
64 analyses (Sourisseau and Carlotti, 2006), while others used the CPR (Continuous Plankton  
65 Recorder) method and were restricted to the “ultra subsurface” (0–7 m) (Beaugrand et al.  
66 2000a, 2000b). Studies with high taxonomic resolution focused on a single field survey

67 (Albaina and Irigoien, 2007; Irigoien et al., 2011) or were conducted on limited spatial scales  
68 despite their large temporal scales (Albaina and Irigoien, 2007; Stenseth et al., 2006; Valdés  
69 and Moral, 1998; Valdés et al., 2007; Gonzalez-Gil et al., 2015; Cabal et al., 2008; Bode et  
70 al., 2012 and 2013). Other studies focused on one or two species on a high spatio-temporal  
71 scale, such as Bonnet et al. (2005) on *Calanus helgolandicus* and Lindley and Daykin (2005)  
72 on *Temora stylifera* and *Centropages chierchiae*. Finally, only two studies were quite similar  
73 to ours, conducting large spatio-temporal surveys of the Bay of Biscay, albeit with a lower  
74 taxonomic resolution (groups were defined by image analysis) (Irigoien et al. 2009;  
75 Vandromme et al. 2014). Irigoien et al. (2009) identified permanent features in the spatial  
76 distribution of spring zooplankton between 1998 and 2006, with a higher abundance of large  
77 organisms over the shelf break and offshore areas. Vandromme et al. (2014) used a  
78 combination of LOPC data and WP2 sampling processed with the Zooscan and employed it  
79 over the same network of stations used in our study between 2005 and 2012. They found a  
80 negative relationship between the zooplankton biomass and normalized biomass size spectra  
81 slopes, thus suggesting a clear association between zooplankton size distribution,  
82 productivity, and transfer efficiency.

83         The novelty of the present study lies in the temporal and spatial coverage of the  
84 mesozooplankton community structure, with a focus on the main mesozooplankton groups  
85 and the key genera or species of copepods. These aspects have not been investigated  
86 previously in the Bay of Biscay. From a large data set of annual spring PELGAS ('PELagique  
87 GAScogne') surveys (Doray et al., this issue), our study aimed to elucidate which drivers  
88 control the spring mesozooplankton community and whether any spatial and/or temporal  
89 changes in this community occurred between 2003 and 2013. We had three objectives: 1) to  
90 summarize the habitat variabilities in terms of temperature, salinity, and chlorophyll *a* data; 2)  
91 to analyze the temporal patterns of the mesozooplankton and copepod spring communities

92 over the studied decade; and 3) to elucidate which local hydrological and trophic variables  
93 may account for the variability of mesozooplankton communities over space and time.

94

## 95 **Materials and Methods**

### 96 **Sampling area**

97 The Bay of Biscay is characterized by a morphostructural dissymmetry opposing the large  
98 northeastern edge of a narrow meridional shelf (Fig. 1). Our study focused on the southern  
99 part of the Armorican shelves, which are largely under the influence of the Gironde and the  
100 Adour river plumes.

### 101 **Data collection**

102 Samples were collected during the annual PELGAS surveys (Doray et al., this volume-b),  
103 which have been conducted every spring since 2000 over the whole continental shelf of the  
104 Bay of Biscay. In this study, we selected a subset of data with a homogenous  
105 mesozooplankton sampling protocol, i.e. data related to the southern part of the Bay of Biscay  
106 from 2000–2013 (Fig. 1). PELGAS surveys routinely collect several parameters for all system  
107 components, including hydrobiology, pelagic fish abundance and distribution, marine  
108 mammals, and seabird observations. We used data that had been collected at night from a total  
109 of 118 visited stations (Table 1). Each station was separated from the next by approximately  
110 44 km in the along-shore direction and 10–25 km in the cross-shelf direction. PELGAS  
111 surveys were not carried out on exactly the same calendar dates over the series (especially at  
112 the beginning of the studied decade), although they always did take place during springtime  
113 over the course of about 15 days (Table 1).

114

115 *Hydrology and phytoplankton biomass*

116 Our station network for hydrology data consisted of 26 to 34 stations per year (Table  
117 1, Fig. 1). At each station, the salinity and temperature were measured over the water column  
118 with a CTD (Seabird 19+v2) probe. Two water column integrated indices were calculated: the  
119 equivalent freshwater depth (m) and the deficit of potential energy or DEP ( $\text{kg}\cdot\text{m}^{-1}\cdot\text{s}^{-2}$ ). As  
120 detailed in Huret et al. (2013), the equivalent freshwater depth represents the local depth of  
121 freshwater in the absence of mixing. As such, equivalent freshwater depth is a good indicator  
122 of the plume influence in a given year and location. The DEP is an index of stratification that  
123 is calculated from the vertical distribution of density values.

124 Chlorophyll *a*-based biomass (*chl<sub>a</sub>*, see Introduction of Boyer et al. 2009) was used as  
125 a proxy of autotrophic biomass (mostly phytoplankton). Water samples (200–500 mL) were  
126 collected with Niskin bottles at the subsurface. Once on board, the samples were passed  
127 through successive filtrations on three membranes with different porosities (Whatman GF/F  
128 with pore sizes of 0.7, 3, and 20  $\mu\text{m}$  and a diameter of 25 mm) to fractionate the samples into  
129 three size classes: pico- (< 3  $\mu\text{m}$ ), nano- (3–20  $\mu\text{m}$ ), and microphytoplankton (>20  $\mu\text{m}$ )  
130 including large taxa such as diatoms. Each sample was stored at  $-20^{\circ}\text{C}$  for subsequent  
131 analysis. Laboratory extraction was performed with a Turner TD-700 fluorometer according  
132 to the protocols of Aminot and K  rouel (2005) and of Lorenzen (1967). The *chl<sub>a</sub>*-based  
133 biomass was expressed in  $\mu\text{g}\cdot\text{L}^{-1}$ . An index of water-column integrated *chl<sub>a</sub>* biomass ( $\mu\text{g}\cdot\text{m}^{-2}$ )  
134 was calculated using the fluorescence data from the vertical profiles (WETStar fluorometer,  
135 WET Labs, USA) and corrected by *chl<sub>a</sub>*-based biomass data.

136

### 137 *Mesozooplankton*

138 The mesozooplankton samples were collected by vertical trawls using WP2 nets (0.25  
139  $\text{m}^2$  opening, 200  $\mu\text{m}$  mesh size), from a depth of 100 m (or the bottom depth for inshore  
140 stations). For each annual survey, ten or 12 stations were selected from four transects; this

141 sampling included coastal, continental shelf, and slope stations (Fig. 1B). After collection, the  
142 net samples were preserved in 4% formaldehyde. The organisms were identified by species,  
143 genus, family, or more general categories/forms (Table 2; identification protocol of Rose  
144 (1933) and Tregoubof and Rose (1957)), and were enumerated using a Leica M3Z stereo  
145 microscope (65× to 100× magnification). The abundance was expressed in individuals m<sup>-3</sup>  
146 (ind.m<sup>-3</sup>).

147

## 148 **Data analysis**

### 149 *Ordinary kriging*

150 To describe the spatio-temporal patterns of the different studied compartments, an  
151 ordinary kriging procedure (ArcMap 10.2 using the Geostatistical Analyst toolbox) was  
152 applied to the data for the subsurface temperature, salinity, and size-fractionated chl $a$ -based  
153 biomass. For each parameter, annual data were compiled from 2003–2013 and interpolated to  
154 provide an overview of the spring spatial patterns over the time series. For each parameter,  
155 annual kriged maps are presented in Supplemental Figures 1–4. To identify significant  
156 temporal variations (i.e., across years) for each parameter (temperature, salinity, and pico-,  
157 nano-, and microphytoplankton biomasses), a non-parametric multiple pairwise comparison  
158 (Statistica®, Tulsa, OK, USA) of mean ranks was applied to all years from 2003–2013; p-  
159 values < 0.05 were considered significant. All other statistical analyses were performed with  
160 the R-Cran project free software (R Core Team, 2014). Furthermore, to consider these five  
161 water mass variables together throughout the decade, confidence ellipses (surrounding the  
162 barycentre of coordinate stations) were determined on a station factor map produced by a  
163 principal component analysis (PCA, ‘FactoMineR’ package (Husson et al., 2012)).

164

### 165 *Mesozooplankton community analysis*



166           The time-variability of the mesozooplankton community was analyzed by considering  
167 the mean yearly relative abundance of classical characteristic groups of mesozooplankton  
168 (meroplankton, gelatinous plankton, copepods, and other holoplankton). The abundance and  
169 taxonomic composition of the dominant group (copepods) was analyzed according to the  
170 variability in space and over time. As done in previous studies, a temporal analysis was  
171 conducted via a multiple comparison of the mean ranks for all years based on copepod  
172 abundance. The spatio-temporal variation in the composition of the adult copepod community  
173 was also described with a non-metric multi-dimensional scaling (NMDS), performed using  
174 Primer 6 (Plymouth Routines In Multivariate Ecological Research) software. A matrix of  
175 sampling points (n=118 samples; see Table 1) was created for the abundance data of copepods  
176 species or genera (n= 23). In this matrix, the columns corresponded to the copepod taxa  
177 abundances, and the lines to the sampling points. The data were transformed with  $\log x + 1$   
178 before the Bray-Curtis metric was applied to estimate the similarity between stations. The  
179 similarity matrix was then ordinated by NMDS. A SIMPER (SIMilarity PERcentage) analysis  
180 was performed to identify the genera or species contributing most to similarity (or  
181 dissimilarity) within (or between) three groups of sampling years defined from the time series  
182 analysis.

183 Finally, to quantify the relative influences of the food-resource (*chl<sub>a</sub>*) and abiotic parameters  
184 (temperature, salinity) that underlie the patterns observed in the copepod community  
185 structure, a variation partitioning analysis (using “vegan” and “ade4” packages in the R-Cran  
186 project free software) was applied (Volis et al., 2011). We considered biotic variables  
187 (subsurface and integrated water column values of *chl<sub>a</sub>* for pico-, nano-, and  
188 microphytoplankton fractions) and abiotic variables (subsurface values of temperature and  
189 salinity, and three water column integrated indices; the DEP, the equivalent fresh water, and  
190 the mixed-layer depth). First the variables to include in the analysis (ie variables that

191 influenced the most the copepod distribution) were selected through forward selection (pack  
192 for package). After the forward selection, two matrices (H matrix for abiotic parameter and C  
193 matrix for biotic parameters) were built using only the most influential variables. Finally,  
194 using these two matrices, the variation partitioning was performed aiming at identifying the  
195 part of technology copepod distribution variation explained by each variable. By this way, our  
196 aim is to evaluate if copepod distribution is better explained by hydrological parameters than  
197 by food resources. Indeed, in ecological matrices each variable has a pure variation and a part  
198 of variation linked to the other variables. This covariation between variables can be evaluated  
199 through the variation partitioning.

200 Variation partitioning evaluates diverse components of variation: 1) the pure effect of  
201 each individual matrix, 2) the redundancy of the two explicative matrices, and 3) the residual  
202 effects that are unexplained by the chosen variables. Redundancy analysis (RDA), partial  
203 redundancy analysis (pRDA), and Monte Carlo permutation (999 permutations) tests were  
204 used to test the significance of the canonical axis.

205

## 206 **Results**

### 207 **Subsurface salinity and temperature**

208 The absence of a spatial pattern in the decadal average map (Fig. 2) means that no  
209 spring-time mesoscale process had a strong recurrent impact on the surface temperature in the  
210 southern Bay of Biscay. However, a coast-to-offshore positive gradient can be observed in  
211 certain years (e.g., in 2006, 2010, and 2013; see Fig. S1), revealing the intermittent  
212 occurrence of an upwelling process along the southern French coast. The Gironde plume  
213 brought characteristically lower temperatures in 2005 and 2006, and a latitudinal gradient also  
214 appeared in some years (e.g., in 2010, 2012, and 2013), albeit without any consistent pattern  
215 across years. These anomalies may be explained by the changing meteorological conditions

216 (e.g., wind, irradiance) during the 15-day survey conduction. During the studied decade  
217 (2003–2013), the subsurface temperature varied from 10.8°C to 19.8°C, highlighting the large  
218 interannual variability in the surface warming and the stratification process during this rapidly  
219 changing season. The non-parametric multiple pairwise comparison allowed for a separation  
220 of the years into three groups: 2003 was the warmest, 2007 and 2011 had intermediate  
221 temperatures, and the remaining years were the coldest (see Fig. S1).

222 The spatial pattern of salinity was driven by the plumes of the Gironde and the Adour  
223 rivers (Fig.2). Despite some interannual variability in the extension of the plumes (maxima in  
224 2007, 2009, and 2013; minima in 2011 and 2012), the interannual variability of the subsurface  
225 salinity was not significantly different between years (multiple pairwise comparison,  $p=0.05$ )  
226 (see Fig. S2). Subsurface salinities varied from 26.07 psu to 36.4 psu (see Fig. S2).

227

### 228 **Chlorophyll *a*-based biomasses**

229 The average picture of the *chl a* biomasses (Fig.2) revealed a homogeneous  
230 concentration over the shelf, with lower values off-shelf, for the two smallest size classes ( $< 3$   
231  $\mu\text{m}$  and  $3\text{--}20 \mu\text{m}$ ). For the largest size class ( $> 20 \mu\text{m}$ ), the highest values were found over a  
232 coastal strip only. Generally, biomasses were higher in the area influenced by the Gironde  
233 plume as compared to the most other southern locations.

234 Substantial differences appeared when analyzing the annual maps of *chl a* biomasses  
235 (see Figs. S3, S4, and S5). For the smallest size class (Fig. S3), significant interannual  
236 differences allowed the years to be divided into five groups: 2003 exhibited the lowest values  
237 ( $0.20 \pm 0.38 \mu\text{g.L}^{-1}$ ) and 2009–2010 exhibited the highest ( $0.66 \pm 0.41 \mu\text{g.L}^{-1}$ ). For the  $3\text{--}20$   
238  $\mu\text{m}$  size class, the interannual variability revealed four groups of years, with mean biomasses  
239 ranging from  $0.17 \pm 0.26 \mu\text{g.L}^{-1}$  to  $0.45 \pm 0.37 \mu\text{g.L}^{-1}$ . For the  $> 20 \mu\text{m}$  size class, no  
240 significant interannual differences were found between years.

241 The non-parametric multiple pairwise comparison of the five environmental variables  
242 (subsurface salinity and temperature, subsurface pico-, nano-, and microphytoplankton  
243 biomasses) over the decade could not extract significant differences between years.

244 The average contribution of each size class over the studied decade (Fig. 3) was 44%  
245 for picophytoplankton ( $< 3 \mu\text{m}$ ), 23% for nanophytoplankton ( $3\text{--}20 \mu\text{m}$ ), and 33% for  
246 microphytoplankton ( $> 20 \mu\text{m}$ ) (Fig. 3). The relative contributions varied from 23% (2003) to  
247 67% (2009) for the picophytoplankton, from 19% (2008) to 42% (2003) for the  
248 nanophytoplankton, and from 10% (2007) to 42% (2008) for the microphytoplankton  
249 (including larger taxa such as diatoms).

250

## 251 **Mesozooplankton**

### 252 *Total abundance and the contribution of the main groups*

253 The mean spring abundance of mesozooplanktonic organisms over the study period  
254 varied from  $1,321 \pm 391 \text{ ind.m}^{-3}$  (2008) to  $4,986 \pm 355 \text{ ind.m}^{-3}$  (2005) (Fig. 4A). Between  
255 2003 and 2006, abundances were higher ( $4,454$ ,  $3,233$ ,  $4,985$ , and  $4,191 \text{ ind.m}^{-3}$  for each year,  
256 respectively) than the mean decadal value ( $2,995 \pm 1,195 \text{ ind.m}^{-3}$ ), while the mean  
257 abundances were lower than the mean decadal value between 2007 and 2013, with the  
258 exceptions of 2010 and 2012 (with  $3,349$  and  $3,061 \text{ ind.m}^{-3}$ , respectively). The spring  
259 abundance of mesozooplanktonic organisms revealed three temporal phases: from 2003–2006  
260 (higher than the mean decadal value), from 2007–2009 (lower than the mean decadal value),  
261 and from 2010–2013 (close to the mean decadal value, except 2011, which was below the  
262 mean decadal value). The lowest contribution of copepods was registered in 2006 (Fig. 4B).  
263 The gelatinous organisms encountered in 2006 were mainly cnidaria and siphonophora as  
264 well as major meroplankton organisms (Bivalvia larvae and Cirripedia). On average, more  
265 than 80% of the spring mesozooplankton community comprised copepods, 8% meroplankton,

266 8% gelatinous plankton, and 4% other holoplanktonic organisms (Fig. 4B). Depending on the  
267 year, the relative abundance of copepods varied from 42% (2006) to 87% (both 2011 and  
268 2009), those of meroplankton from 1% (2009) to 22% (2006), those of gelatinous organisms  
269 from 3% (2011) to 24% (2006), and those of the other holoplanktonic organisms from 2%  
270 (2009) to 11% (2010). Meroplanktonic organisms were found mostly along the coast,  
271 gelatinous organisms were scattered, and the other holoplanktonic organisms were widespread  
272 among the sampling stations (data not shown). Based on these observations, the following  
273 results focus on the main group: the copepods.

274

#### 275 *Copepod patterns*

276 Over the 11 springtime surveys, copepodites (16% of the total copepod abundance)  
277 and nauplii (1.4%) of miscellaneous copepod species were recorded.

278 Twenty-five adult copepod taxa (at the family, genus, or species level) were recorded;  
279 orders included Harpacticoida, Poecilostomatoida, Cyclopoida, and Calanoida, as well as  
280 copepodites and copepod nauplii (Table 2). The spatial distribution of these 25 taxa is shown  
281 in Fig. 5. Irrespective of the year, the copepod abundance followed a longitudinal gradient:  
282 coastal waters had the highest values ( $2,848 \pm 2,507 \text{ ind.m}^{-3}$ ), shelf waters had intermediate  
283 values ( $2,335 \pm 3,787 \text{ ind.m}^{-3}$ ), and the continental slope had the lowest values ( $1,304 \pm 1,546$   
284  $\text{ind.m}^{-3}$ ), except for in 2010 ( $1,467 \text{ ind.m}^{-3}$ ). One outlier of copepod abundance ( $21,127 \text{ ind.m}^{-3}$ )  
285 was recorded in 2005 at a single station on the northern coast. From a temporal viewpoint  
286 and based on the annual abundances at each station, only 2009 could be distinguished from  
287 the other years (Fig. S6). Moreover, eight of these 25 adult taxa (*Oithona* spp., *Acartia* spp.,  
288 *Temora longicornis*, *Oncaea* spp., Calanidae, *Calanus helgolandicus*, Paracalanidae, and  
289 *Euterpina acutifrons*) alone represented more than 1.5% of the copepod abundance (Table 2).  
290 Their spring spatial abundances in the Bay of Biscay are plotted in Fig. 5. *Oithona* spp. was

291 present preferentially from the continental shelf to the slope; *Acartia* spp., *Oncaea* spp., and  
292 *Temora longicornis* were most common at the coastal stations; and the genera *Acartia*,  
293 *Oithona*, *Temora*, and *Oncaea* were the most abundant within the copepod community (66%  
294 between 2003 and 2013; see details in Table 2).

295

#### 296 *Spatio-temporal variations of adult copepods*

297 The NMDS ordination of the adult copepod abundance data (stress value of 0.23,  
298 indicating a good ordination) discriminated the temporal variations better than the spatial  
299 variations. The plots of the three time-sampling groups previously discerned by the temporal  
300 analysis of abundance (see above) showed that the adult copepod community in the 2003–  
301 2006 period was clearly distinct from the 2007–2009 period (Fig. 6). The last period (2010–  
302 2013) was intermediate, suggesting a return toward the initial situation (2003–2006) (Fig. 6).  
303 The SIMPER analysis (Tables 3 and 4) confirmed this trend, with the same four taxa (*Oithona*  
304 spp., *Oncaea* spp., *Acartia* spp., and *Temora longicornis*) explaining > 65% of the similarity  
305 within the 2003–2006 and 2010–2013 periods, whereas in 2007–2009, Paracalanidae (15%  
306 contribution for this group) replaced *Temora longicornis* (7.8%) in these top-four taxa.  
307 Overall, the within-group similarity was higher for the 2003–2006 (67.0%) and the 2010–  
308 2013 (59.9%) periods than for the 2007–2009 period (52.3%). The level of dissimilarity  
309 between the groups was highest between 2003–2006 and 2007–2009 (52.0%), and lowest  
310 between 2003–2006 and 2010–2013 (45.5%).

311

#### 312 *Hydrological versus trophic control on the spring copepod community*

313 The forward selection identified four significant variables that significantly drive the copepod  
314 distribution: microphytoplankton (> 20 µm) biomass at the subsurface, equivalent freshwater  
315 height, DEP, and subsurface temperature (Table 5). The variation partitioning highlighted that

316 49.2% of the variation was explained by both matrices H and C with the most variance  
317 (24.3%) attributable to chl $a$ -based microphytoplankton biomass and the next-most variance  
318 (13.7%) attributable to hydrological parameters (Figure 7, Supplemental table 1). The part of  
319 the variation due by the interaction between the 2 matrices (ie. between hydrological  
320 parameters and subsurface microphytoplankton) was 11.2 %. Partial RDA (without  
321 interaction between variables) concurred that the distribution of the copepod community was  
322 influenced significantly by the microphytoplankton subsurface biomass, equivalent freshwater  
323 height, and DEP (Supplemental table 1). The contribution of the subsurface temperature was  
324 not significant in the variation partitioning analysis.

325

## 326 **Discussion**

### 327 *Hydrological and biological features of the mesozooplankton habitat*

328 Throughout the 2003–2013 decade, surface water warming occurred continually in the  
329 Bay of Biscay, from the south to the north and from the coast to the open sea. The water mass  
330 circulation in the Bay of Biscay is driven by a combination of large-scale and local forces (Le  
331 Boyer et al., 2013); the warming of water masses in spring is modulated by slope currents,  
332 shelf residual circulation, and the Iberian Poleward Current from Galicia to the Bay of Biscay  
333 on a larger scale, and wind and irradiance conditions on a local scale (Koutsikopoulos and Le  
334 Cann, 1996; Puillat et al., 2004; Rubio et al., 2013). From our study, the spatial pattern of  
335 variability in the south of the Bay appeared to be independent of the interannual variability of  
336 the hydrobiological parameters (e.g., the subsurface temperature). From 2003–2013, the  
337 survey observed a mix of warm (in 2003, 2007, and 2011), intermediate, and cold years. This  
338 variation in temperature regimes is consistent with results previously reported in this area  
339 (e.g., Huret et al., 2013).

340           The size structure of the phytoplankton community contribute to the structure of  
341 pelagic food webs, so our study considered three size classes (pico-, nano-, and  
342 microphytoplankton). Indeed, mesozooplanktonic organisms are major grazers of nano- and  
343 microphytoplankton (Marquis et al., 2007). Calvo-Díaz et al. (2008) recorded the monthly  
344 contributions (in Iberian Peninsula waters from 2003–2006) of each size fraction of  
345 phytoplankton, and showed that the spring (i.e., April) contribution of picophytoplankton was  
346 about 20%, corresponding to the minimum recorded over an annual cycle. By contrast, the  
347 contributions of nanophytoplankton and microphytoplankton were around 50% and 30%,  
348 respectively. In our study, the mean balance between pico- and nanophytoplankton varied  
349 widely, most likely because our spatial coverage involved more oceanic features beyond  
350 200 m of bathymetry. It is important to note that the survey dates were not exactly the same  
351 throughout the decade and hence added further variability. For example, compared to the later  
352 surveys, the 2003 survey captured significantly different hydrology, plankton concentration,  
353 and size structure.

354           To summarize, taking into account both the hydrological and the phytoplanktonic  
355 components of the mesozooplankton habitat, the Bay of Biscay appeared to support a  
356 consistent spatial structure across years, due mainly to the continental supply of freshwater  
357 and nutrients, although a degree of interannual variability occurred in the range of the  
358 observed values.

359

#### 360           *The spring mesozooplankton community*

361           Among the prominent groups of the mesozooplankton community, meroplanktonic  
362 organisms were restricted to the coastal area in our study, as previously reported by Ayata et  
363 al. (2011). By contrast, gelatinous organisms were dispersed throughout the Bay of Biscay.  
364 No clear spatio-temporal development of gelatinous plankton was observed, although this



365 group (mainly cnidaria and siphonophora) was particularly abundant in 2006. Their  
366 proliferation may be linked to climate change, eutrophication, and/or habitat modifications  
367 (e.g., Lo et al., 2008). However, the WP2 net used in the study probably was not the most  
368 suitable device for monitoring gelatinous plankton.

369 In the present study, copepods represented the most dominant holoplankton taxa of the  
370 mesozooplankton community, as highlighted by various studies in the same area (e.g.,  
371 Albaina and Irigoien, 2007; Irigoien et al., 2009; Valdés et al., 2007; Villate et al., 2014,  
372 1997). Previous observations of the spatial distribution of the spring size structure of  
373 mesozooplankton have reported a negative coastal-to-offshore gradient (e.g., Vandromme et  
374 al., 2014), as also observed in the present study for copepod taxa. Here, the sample  
375 represented three dominant genera and one dominant species (> 10% of the copepod  
376 abundance) *Acartia* spp., *Oncaea* spp., *Oithona* spp., and *Temora longicornis*—consistent  
377 with previous investigations (e.g., Albaina and Irigoien, 2007; Irigoien et al., 2011).  
378 According to the literature regarding the copepod community in the Bay of Biscay, *Temora*  
379 *longicornis* and *Pseudocalanus elongatus* are dominant neritic species that occur  
380 preferentially on the continental shelf, whereas *Acartia* spp. dominates stations under coastal  
381 influence, and *Calanus helgolandicus* and *Eucalanidae* dominate under oceanic influence.  
382 More specifically, *C. helgolandicus* is found in the southern part of the Bay of Biscay and in  
383 the surface layers in the north during the spring (Bonnet et al. 2005).

384

#### 385 *Temporal trends in the mesozooplankton and copepod communities*

386 Climatic indicators increasingly are being explored to identify major changes affecting  
387 plankton (e.g., Wouters et al., 2015) and fish communities (Guénette and Gascuel, 2012). On a  
388 similar spatial scale as in the present study, previous research detected oscillations mainly in  
389 the vicinity of the Gironde river plume, which represents a major source of nutrient inputs

390 into the Bay of Biscay for both plankton (David et al., 2005) and fish (Pasquaud et al., 2012).  
391 Overall temperatures in the Gironde estuary increased significantly around 1987 and again  
392 around 2001 (Chaalali et al., 2013).

393         During the decade studied here, the year 2005 brought additional abrupt changes in  
394 mesozooplankton abundance and diversity in the Gironde estuary—a relatively closed  
395 system—and in the Arcachon basin (Chaalali, personal communication). It is possible that  
396 this abrupt change also occurred in the Bay of Biscay, albeit with a time lag that is linked to  
397 the Bay’s resilience properties. As described above, three temporal phases of adult copepod  
398 dominance were observed in the present study: 2003–2006, 2007–2009, and 2010–2013, with  
399 abundance values that were higher, lower, and higher, respectively, than the spring mean  
400 decadal abundance (including 2003–2013). This temporal oscillation also correlated with  
401 taxonomic composition changes (see Tables 3 and 4). However, we observed that 2010–2013  
402 witnessed a reversal to the initial situation (2003–2006) with regard to both the abundance  
403 and taxonomic composition of the adult copepod community. The only anomaly detected was  
404 the high percentage of gelatinous organisms in the spring of 2006, which correlated with the  
405 low percentage of copepods observed that year. These gelatinous organisms comprised  
406 cnidaria and siphonophora primarily. It is reasonable to consider predation as a possible  
407 cause, as this would result in top-down control on copepods and spatial occupation of a very  
408 close ecological niche between carnivorous copepods, cnidarian, and siphonophora  
409 organisms.

410

#### 411         *Factors controlling the spring copepod community*

412         The structure and functioning of planktonic food webs depend largely on the  
413 hydrodynamics of the water column. Our study found that four variables of the pelagic habitat  
414 (subsurface temperature, stratification with the deficit of potential energy, equivalent

415 freshwater height, and subsurface microphytoplankton biomass) accounted for more than 49%  
416 of the variability in the main mesozooplanktonic community. Zarauz et al. (2008) suggested  
417 that the mesozooplankton biomass is driven mainly by hydrogeographic data (e.g., latitude,  
418 longitude, surface temperature, salinity, stratification index, and water depth), and to a lesser  
419 extent by potential trophic resources (e.g., the nano-microplankton biomass). By contrast, the  
420 present study showed that for the same study site (same scale and season), the spring copepod  
421 community (described taxonomically) was influenced more by trophic variables (e.g.,  
422 microphytoplankton biomass; 24.3% of the total variability) than by hydrographic variables  
423 (13.7% of the total variability) over the 11-year time period. These differences can be  
424 explained by the fact that Zarauz et al. (2008) studied mesozooplankton at the biomass level  
425 only, whereas our study took into account the abundance of taxa (species, gender, or family)  
426 to describe the community. These methods do not provide the same ecological information.  
427 Moreover, the temporal dataset was not exactly the same: Zarauz et al. (2008) studied three  
428 spring seasons (2004–2006) while the present study included eleven spring seasons (2003–  
429 2013). Finally, the two studies used different trophic variables for the statistical analysis:  
430 nano-microplankton biomass in Zarauz et al. (2008) vs. phytoplankton biomasses by size  
431 classes in the present study.

432         At the scale and with the spring timing of our study, the trophic link (i.e., the  
433 subsurface microphytoplankton biomass) appeared to be the major driver of the copepod  
434 community, while hydrographic variables appeared to play less important roles. There are two  
435 potential reasons for this: i) the trophic dimension probably represents a time integration of  
436 hydrological conditions (i.e., more integrated than the temperature and salinity variables in the  
437 present context), and ii) the planktonic food web probably has an ecological succession of  
438 physical and geographical parameters that control the initial phytoplanktonic blooms in late  
439 winter. Nutrients then become limited in spring, ultimately influencing the production and life

440 cycle of mesozooplankton, which thus are maintained by trophic control during the PELGAS  
441 spring surveys. However, copepods have other potential trophic sources, such as ciliates and  
442 heterotrophic flagellates, that can influence the mesozooplankton distribution but were not  
443 considered in our study.

444         According to the present observations, both the thermal stratification and equivalent  
445 freshwater height significantly affected the copepod community, whereas subsurface salinity  
446 did not. This probably is because thermal stratification and equivalent freshwater height are  
447 more integrated spatially and temporally. However, it is surprising the water column  
448 integrated chl $a$  index did not have a prominent effect in the non-parametric multiple pairwise  
449 comparison of mean ranks. Thus, an approach using functional traits appears to be more  
450 efficient for understanding the springtime copepod community, as copepods are major  
451 predators of microphytoplankton (Marquis et al., 2007). Moreover, although fewer stations  
452 were sampled in our study than in Irigoien et al. (2011), we explained a greater percentage of  
453 the community's variability, probably because our data set spanned a longer period of time  
454 and therefore captured more variability. However, half of the variation in the copepod  
455 community over the studied decade remained unexplained. We concur with Irigoien et al.  
456 (2011) that other biological functional traits of the present community—including the effect  
457 of copepod density on feeding activities—merit consideration.

458

#### 459         *Concluding remarks*

460         This study of annual springtime PELGAS survey data is the only analysis of the southern  
461 Bay of Biscay's mesozooplankton community between 2003 and 2013. We claim the  
462 following contributions:

- 463       • We demonstrated that the spatial structure found in the Bay of Biscay is attributable to  
464           continental outflow, although some interannual variability occurred in the range of  
465           the values observed.
- 466       • We generated interpolation maps that represent a valuable foundation for future  
467           studies in the Bay of Biscay.
- 468       • We identified three time-oscillation phases (in terms of both abundance and taxonomic  
469           composition) in the mesozooplankton community, with a major change recorded in  
470           2006.
- 471       • We demonstrated, for the first time in this area, the influence of trophic variables (i.e.,  
472           microphytoplankton biomass) from 2003–2013.

473

#### 474 **Acknowledgments**

475 We thank the entire PELGAS team – researchers, technicians, students, captains and crews of  
476 R/V “Thalassa” – who have contributed to the collection of the PELGAS samples since 2003.  
477 We would like to express our thanks to two teams’ laboratory, LIENSs and EMH and  
478 especially, M. Jacques, P. Petitgas, M. Doray, and P. Bourriau. We are grateful to Proof-  
479 reading and Dr. Sophie Domingues-Montanari for English corrections. We also grateful to  
480 Céline Lavergne for its statistical advices. The IUF (Institut Universitaire de France) is  
481 acknowledged for its support to PB as a Senior Member. This research was supported through  
482 a PhD grant for A. Dessier from the Conseil Régional de Poitou-Charentes and by the  
483 European project REPRODUCE (EraNet-Marifish, FP7). This work was supported by the  
484 “Plateau Microscopie” of the LIENSs laboratory.

- 486 Albaina, A., Irigoien, X., 2007. Fine scale zooplankton distribution in the Bay of Biscay  
487 in spring 2004. *J. Plankton Res.* 29, 851–870. doi:10.1093/plankt/fbm064
- 488 Aminot, A., K erouel, R., 2005. Hydrologie des  cosyst mes marins. Param tres et  
489 analyses., Ifremer. ed, M thodes d’analyses du milieu marin.
- 490 Ayata, S.-D., Stolba, R., Comtet, T., Thi baut,  ., 2011. Meroplankton distribution and  
491 its relationship to coastal mesoscale hydrological structure in the northern Bay of Biscay (NE  
492 Atlantic). *J. Plankton Res.* 33, 1193–1211. doi:10.1093/plankt/fbr030
- 493 Batchelder, H.P., Mackas, D.L., O’Brien, T.D., 2012. Spatial–temporal scales of  
494 synchrony in marine zooplankton biomass and abundance patterns: A world-wide  
495 comparison. *Glob. Comp. Zooplankton Time Ser.* 97–100, 15–30.  
496 doi:10.1016/j.pocean.2011.11.010
- 497 Beaugrand, G., Brander, K.M., Lindley, J.A., Souissi, S., Reid, P.C., 2003. Plankton  
498 effect on cod recruitment in the North Sea. *Nature* 426, 661–664. doi:10.1038/nature02164
- 499 Beaugrand, G., Iba nez, F., Lindley, J.A., Reid, P.C., 2002. Diversity of calanoid  
500 copepods in the North Atlantic and adjacent seas: Species associations and biogeography.  
501 *Mar. Ecol. Prog. Ser.* 232, 179–195. doi:10.3354/meps232179
- 502 Beaugrand, G., Ibanez, F., Reid, P.C., 2000a. Spatial, seasonal and long-term fluctuations  
503 of plankton in relation to hydroclimatic features in the English Channel, Celtic Sea and Bay of  
504 Biscay. *Mar. Ecol. Prog. Ser.* 200, 93–102.
- 505 Beaugrand, G., Reid, P.C., Iba nez, F., Planque, B., 2000b. Biodiversity of North Atlantic  
506 and North Sea calanoid copepods. *Mar. Ecol. Prog. Ser.* 204, 299–303.
- 507 Bode, A., Alvarez-Ossorio, M., Miranda, A., L pez-Urrutia, A., Vald s, L., 2012.  
508 Comparing copepod time-series in the north of Spain: Spatial autocorrelation of community  
509 composition. *Prog. Oceanogr.* 97–100, 108–119. doi:10.1016/j.pocean.2011.11.013
- 510 Bode, A.,  lvarez-Ossorio, M.T., Miranda, A., Ruiz-Villarreal, M., 2013. Shifts between  
511 gelatinous and crustacean plankton in a coastal upwelling region. *ICES J. Mar. Sci.* 70, 934–  
512 942. doi:10.1093/icesjms/fss193
- 513 Bonnet, D., Richardson, A., Harris, R., Hirst, A., Beaugrand, G., Edwards, M., 2005. An  
514 overview of *Calanus helgolandicus* ecology in European waters. *Prog. Oceanogr.* 65, 1–53.  
515 doi:10.1016/j.pocean.2005.02.002
- 516 Boyer, J.N., Kelble, C.R., Ortner, P.B., Rudnick, D.T., 2009. Phytoplankton bloom  
517 status: Chlorophyll a biomass as an indicator of water quality condition in the southern  
518 estuaries of Florida, USA. *Ecol. Indic.* 9, S56–S67. doi:10.1016/j.ecolind.2008.11.013
- 519 Cabal, J., Gonz lez-Nuevo, G., Nogueira, E., 2008. Mesozooplankton species distribution  
520 in the NW and N Iberian shelf during spring 2004: Relationship with frontal structures. *J.*  
521 *Mar. Syst.* 72, 282–297. doi:10.1016/j.jmarsys.2007.05.013
- 522 Calvo-D az, A., Mor n, X.A.G., Su rez, L. ., 2008. Seasonality of picophytoplankton  
523 chlorophyll a and biomass in the central Cantabrian Sea, southern Bay of Biscay. *J. Mar. Syst.*  
524 72, 271–281. doi:10.1016/j.jmarsys.2007.03.008
- 525 Chaalali, A., Beaugrand, G., Bo t, P., Sautour, B., 2013. Climate-Caused Abrupt Shifts in  
526 a European Macrotidal Estuary. *Estuaries Coasts* 36, 1193–1205. doi:10.1007/s12237-013-  
527 9628-x
- 528 Childs, C., 2004. Interpolating Surfaces in ArcGIS Spatal Analyst - interpolating.pdf.  
529 ESRI Educ. Serv. ArcUser.
- 530 Doray Mathieu, Petitgas Pierre, Huret Martin, Duhamel Erwan, Romagnan Jean-Baptiste,  
531 Authier Matthieu, Dupuy Christine, Spitz Jerome. this volume-a. Monitoring small pelagic  
532 fish in the Bay of Biscay ecosystem, using indicators from an integrated survey . *Progress in*  
533 *Oceanography* IN PRESS . <http://doi.org/10.1016/j.pocean.2017.12.004>

534 Doray, M., Petitgas, P., Romagnan, J.B., Huret, M., Duhamel, E., Dupuy, C., Spitz, J.,  
535 Authier, M., Sanchez, F., Berger, L., Dorémus, G., Bourriau, P., Grellier, P., Massé, J., this  
536 volume-b. The PELGAS survey: ship-based integrated monitoring of the Bay of Biscay  
537 pelagic ecosystem. *Prog. Oceanogr.*

538 González, M., Fontán, A., Esnaola, G., Collins, M., 2013. Abrupt changes, multidecadal  
539 variability and long-term trends in sea surface temperature and sea level datasets within the  
540 southeastern Bay of Biscay. *XII Int. Symp. Oceanogr. Bay Biscay* 109–110, Supplement,  
541 S144–S152. doi:10.1016/j.jmarsys.2011.11.014

542 Guénette, S., Gascuel, D., 2012. Shifting baselines in European fisheries: The case of the  
543 Celtic Sea and Bay of Biscay. *Spec. Issue Fish. Policy Reform EU* 70, 10–21.  
544 doi:10.1016/j.ocecoaman.2012.06.010

545 Hinder, S.L., Gravenor, M.B., Edwards, M., Ostle, C., Bodger, O.G., Lee, P.L.M., Walne,  
546 A.W., Hays, G.C., 2014. Multi-decadal range changes vs. thermal adaptation for north east  
547 Atlantic oceanic copepods in the face of climate change. *Glob. Change Biol.* 20, 140–146.  
548 doi:10.1111/gcb.12387

549 Huret, M., Sourisseau, M., Petitgas, P., Struski, C., Léger, F., Lazure, P., 2013. A multi-  
550 decadal hindcast of a physical–biogeochemical model and derived oceanographic indices in  
551 the Bay of Biscay. *XII Int. Symp. Oceanogr. Bay Biscay* 109–110, Supplement, S77–S94.  
552 doi:10.1016/j.jmarsys.2012.02.009

553 Huret M, Bourriau P, Doray M, Gohin F, Petitgas P (2018) Survey timing vs. ecosystem  
554 scheduling: Degree-days to underpin observed interannual variability in marine ecosystems.  
555 *Prog Oceanogr*, In Press.

556 [Husson, F., Josse, J., Le, S. & Mazet, J. \(2012\) FactoMineR: Multivariate Exploratory](#)  
557 [Data Analysis and Data Mining with R. R package version 1.18](#) Irigoien, X., Chust, G.,  
558 Fernandes, J.A., Albaina, A., Zarauz, L., 2011. Factors determining the distribution and  
559 beta diversity of mesozooplankton species in shelf and coastal waters of the Bay of Biscay. *J.*  
560 *Plankton Res.* 33, 1182–1192. doi:10.1093/plankt/fbr026

561 Irigoien, X., Fernandes, J.A., Grosjean, P., Denis, K., Albaina, A., Santos, M., 2009.  
562 Spring zooplankton distribution in the Bay of Biscay from 1998 to 2006 in relation with  
563 anchovy recruitment. *J. Plankton Res.* 31, 1–17. doi:10.1093/plankt/fbn096

564 Koutsikopoulos, C., Le Cann, B., 1996. Physical processes and hydrological structures  
565 related to the Bay of Biscay anchovy. *Sci. Mar.* 60, 9–19.

566 Lassalle, G., Chouvelon, T., Bustamante, P., Niquil, N., 2014. An assessment of the  
567 trophic structure of the Bay of Biscay continental shelf food web: Comparing estimates  
568 derived from an ecosystem model and isotopic data. *Prog. Oceanogr.* 120, 205–215.  
569 doi:10.1016/j.pocean.2013.09.002

570 Le Boyer, A., Charria, G., Le Cann, B., Lazure, P., Marié, L., 2013. Circulation on the  
571 shelf and the upper slope of the Bay of Biscay. *Cont. Shelf Res.* 55, 97–107.  
572 doi:10.1016/j.csr.2013.01.006

573 Legendre, L., Le Fèvre, J., 1991. From Individual Plankton Cells To Pelagic Marine  
574 Ecosystems And To Global Biogeochemical Cycles, in: Demers, S. (Ed.), *Particle Analysis in*  
575 *Oceanography*, NATO ASI Series. Springer Berlin Heidelberg, pp. 261–300.

576 Lindley, J.A., Daykin, S., 2005. Variations in the distributions of *Centropages chierchiae*  
577 and *Temora stylifera* (Copepoda: Calanoida) in the north-eastern Atlantic Ocean and western  
578 European shelf waters. *ICES J. Mar. Sci.* 62, 869–877. doi:10.1016/j.icesjms.2005.02.009

579 Lo, W.-T., Purcell, J.E., Hung, J.-J., Su, H.-M., Hsu, P.-K., 2008. Enhancement of  
580 jellyfish (*Aurelia aurita*) populations by extensive aquaculture rafts in a coastal lagoon in  
581 Taiwan. *Ices J. Mar. Sci.* 65, 453–461. doi:10.1093/icesjms/fsm185

582 Lorenzen, C.J., 1967. Determination of chlorophyll and pheopigments:  
583 spectrophotometric equations. *Limnol. Oceanogr.* 12, 343–346.

584 Marquis, E., Niquil, N., Delmas, D., Hartmann, H.J., Bonnet, D., Carlotti, F., Herbland,  
585 A., Labry, C., Sautour, B., Laborde, P., Vézina, A., Dupuy, C., 2007. Inverse analysis of the  
586 planktonic food web dynamics related to phytoplankton bloom development on the  
587 continental shelf of the Bay of Biscay, French coast. *Estuar. Coast. Shelf Sci.* 73, 223–235.  
588 doi:10.1016/j.ecss.2007.01.003

589 Motos, L., 1996. Reproductive biology and fecundity of the Bay of Biscay anchovy  
590 population (*Engraulis encrasicolus* L.). *Sci. Mar.* 60, 195–207.

591 O'Brien, T.D., Wiebe, P.H., Falkenhaus, T., 2013. ICES Zooplankton Status Report  
592 2010/2011 (No. 318). ICES Cooperative Research Report.

593 Pasquaud, S., Béguer, M., Larsen, M.H., Chaalali, A., Cabral, H., Lobry, J., 2012.  
594 Increase of marine juvenile fish abundances in the middle Gironde estuary related to warmer  
595 and more saline waters, due to global changes. *Estuar. Coast. Shelf Sci.*  
596 doi:10.1016/j.ecss.2012.03.021

597 Perry, R.I., Batchelder, H.P., Mackas, D.L., Chiba, S., Durbin, E., Greve, W., Verheye,  
598 H.M., 2004. Identifying global synchronies in marine zooplankton populations: Issues and  
599 opportunities. *ICES J. Mar. Sci.* 61, 445–456. doi:10.1016/j.icesjms.2004.03.022

600 Planque, B., Bellier, E., Jégou, A.M., Lazure, P., Puillat, I., 2003. Large scale  
601 hydroclimatic variability in the Bay of Biscay. The 1990s in the context of interdecadal  
602 changes. *ICES Mar. Sci. Symp.* 219, 61–70.

603 Puillat, I., Lazure, P., Jégou, A., Lampert, L., Miller, P., 2004. Hydrographical  
604 variability on the French continental shelf in the Bay of Biscay, during the 1990s. *Cont. Shelf*  
605 *Res.* 24, 1143–1163. doi:10.1016/j.csr.2004.02.008

606 Puillat, I., Lazure, P., Jégou, A., Planque, B., Lampert, L., 2003. Mesoscale, interannual,  
607 and Seasonal hydrological variability over the French continental shelf of the Bay of Biscay  
608 during the 1990s. *ICES Mar. Sci. Symp.* 219, 333–336.

609 R Core Team, 2014. R: A language and environment for statistical computing. R Found.  
610 *Stat. Comput.* Vienna Austria.

611 Richardson, A.J., 2008. In hot water: zooplankton and climate change. *ICES J. Mar. Sci.*  
612 *J. Cons.* 65, 279–295. doi:10.1093/icesjms/fsn028

613 Rose, M., 1933. Faune de France - Copépodes Pélagiques, Fédération française des  
614 sociétés des sciences naturelles - Office central de Faunistique.

615 Rubio, A., Fontán, A., Lazure, P., González, M., Valencia, V., Ferrer, L., Mader, J.,  
616 Hernández, C., 2013. Seasonal to tidal variability of currents and temperature in waters of the  
617 continental slope, southeastern Bay of Biscay. *XII Int. Symp. Oceanogr. Bay Biscay* 109–110,  
618 *Supplement*, S121–S133. doi:10.1016/j.jmarsys.2012.01.004

619 Sourisseau, M., Carlotti, F., 2006. Spatial distribution of zooplankton size spectra on the  
620 French continental shelf of the Bay of Biscay during spring 2000 and 2001. *J. Geophys. Res.*  
621 *Oceans* 111, 12. doi:10.1029/2005JC003063

622 Stenseth, N.C., Llope, M., Anadon, R., Ciannelli, L., Chan, K.-S., Hjermmann, D.O.,  
623 Bagoien, E., Ottersen, G., 2006. Seasonal plankton dynamics along a cross-shelf gradient.  
624 *Proc. R. Soc. B Biol. Sci.* 273, 2831–2838. doi:10.1098/rspb.2006.3658

625 Tregoubof, G., Rose, M., 1957. *Le manuel de planctonologie méditerranéenne*, Centre  
626 National de la Recherche Scientifique. Paris.

627 Valdés, L., López-Urrutia, A., Cabal, J., Alvarez-Ossorio, M., Bode, A., Miranda, A.,  
628 Cabanas, M., Huskin, I., Anadón, R., Alvarez-Marqués, F., 2007. A decade of sampling in the  
629 Bay of Biscay: What are the zooplankton time series telling us? *Prog. Oceanogr.* 74, 98–114.  
630 doi:10.1016/j.pocean.2007.04.016

631 Valdés, L., Moral, M., 1998. Time-series analysis of copepod diversity and species  
632 richness in the southern Bay of Biscay off Santander, Spain, in relation to environmental  
633 conditions. *ICES J. Mar. Sci. J. Cons.* 55, 783–792. doi:10.1006/jmsc.1998.0386



634 Vandromme, P., Nogueira, E., Huret, M., Lopez-Urrutia, Á., González-Nuevo González,  
635 G., Sourisseau, M., Petitgas, P., 2014. Springtime zooplankton size structure over the  
636 continental shelf of the Bay of Biscay. *Ocean Sci.* 10, 821–835. doi:10.5194/os-10-821-2014  
637 Villate, F., Moral, M., Valencia, V., 1997. Mesozooplankton community indicates  
638 climate changes in a shelf area of the inner Bay of Biscay throughout 1988 to 1990. *J.*  
639 *Plankton Res.* 19, 1617–1636.  
640 Villate, F., Uriarte, I., Olivar, M.P., Maynou, F., Emelianov, M., Ameztoy, I., 2014.  
641 Mesoscale structure of microplankton and mesoplankton assemblages under contrasting  
642 oceanographic conditions in the Catalan Sea (NW Mediterranean). *J. Mar. Syst.* 139, 9–26.  
643 doi:10.1016/j.jmarsys.2014.05.004  
644 Volis, S., Dorman, M., Blecher, M., Sapir, Y., Burdeniy, L., 2011. Variation partitioning  
645 in canonical ordination reveals no effect of soil but an effect of co-occurring species on  
646 translocation success in *Iris atrofusca*. *J. Appl. Ecol.* 48, 265–273. <http://dx.doi.org/10.1111/j.1365-2664.2010.01898.x>.  
647  
648 Wouters, N., Dakos, V., Edwards, M., Serafim, M.P., Valayer, P.J., Cabral, H.N., 2015.  
649 Evidencing a regime shift in the North Sea using early-warning signals as indicators of critical  
650 transitions. *Estuar. Coast. Shelf Sci.* 152, 65–72. doi:10.1016/j.ecss.2014.10.017  
651 Zarauz, L., Irigoien, X., Fernandes, J.A., 2008. Modelling the influence of abiotic and  
652 biotic factors on plankton distribution in the Bay of Biscay, during three consecutive years  
653 (2004–06). *J. Plankton Res.* 30, 857–872. doi:10.1093/plankt/fbn049  
654

655 **List of Figures**

656 **Figure 1:** Map of the Bay of Biscay showing the location of the sampling stations of A) sub-  
657 surface water environmental parameters (temperature, salinity, size-fractionated biomass of  
658 chlorophyll *a*), and B) the mesozooplankton community. Isobaths 100 m (dotted line), 200 m  
659 (solid line) and 500 m (dashed line) are drawn.

660 **Figure 2:** Results of the annual (2003-2013) spatial interpolation of sub-surface temperature  
661 (°C), salinity (psu), picophytoplankton ( $chl a < 3 \mu m$ ) biomass, nanophytoplankton ( $3 \mu m$   
662  $< chl a < 20 \mu m$ ), and microphytoplankton ( $chl a > 20 \mu m$ ) biomass ( $\mu g \cdot L^{-1}$ ) in the southern Bay  
663 of Biscay.

664 **Figure 3:** Interannual variation of the mean relative biomass of surface size-fractionated  
665 chlorophyll *a* between 2003 and 2013 in the southern Bay of Biscay; in black for the  
666 picophytoplankton biomass ( $< 3 \mu m$ ), in light grey for the nanophytoplankton biomass ( $3-$   
667  $20 \mu m$ ) and in dark grey ( $> 20 \mu m$ ) for the microphytoplankton biomass.

668 **Figure 4:** Interannual variation of the mesozooplankton abundance between 2003 and 2013:  
669 A) mean decadal and annual abundances ( $ind \cdot m^{-3} \pm SD$ ) of the entire mesozooplankton  
670 community and, B) stacked bar charts presenting the relative abundance of identified  
671 organisms belonging to copepods, gelatinous, other holoplankton and meroplankton groups  
672 on both the annual and decadal scale.

673 **Figure 5:** Annual spatial distribution of abundance ( $ind \cdot m^{-3}$ ) for major families, genera or  
674 species contributing for more than 1.5% in abundance to the copepods community between  
675 2003 and 2013 in the southern Bay of Biscay. The size of the pies is proportional to the total  
676 from each station throughout the decade.

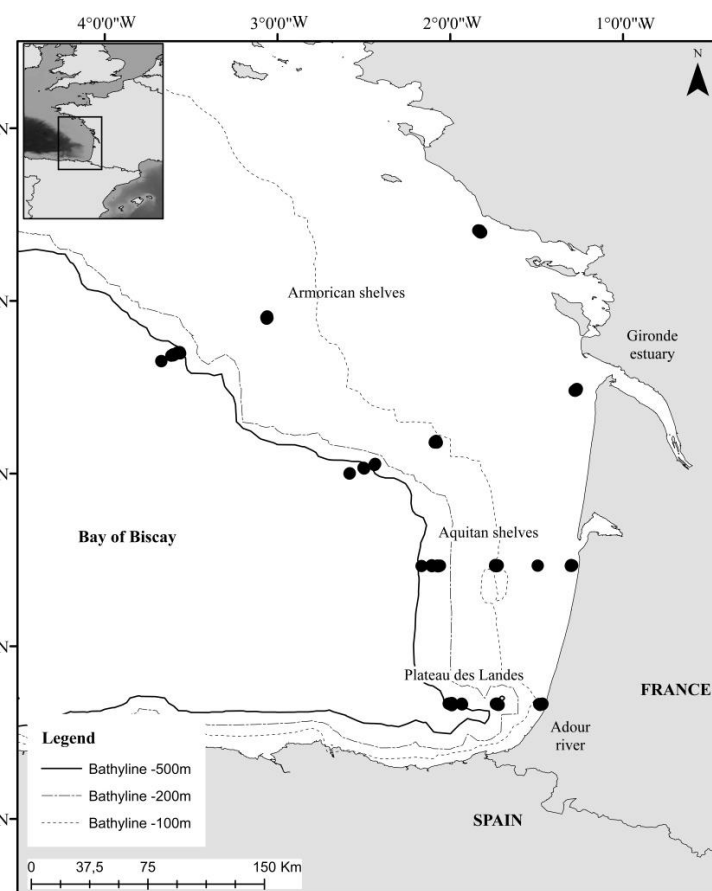
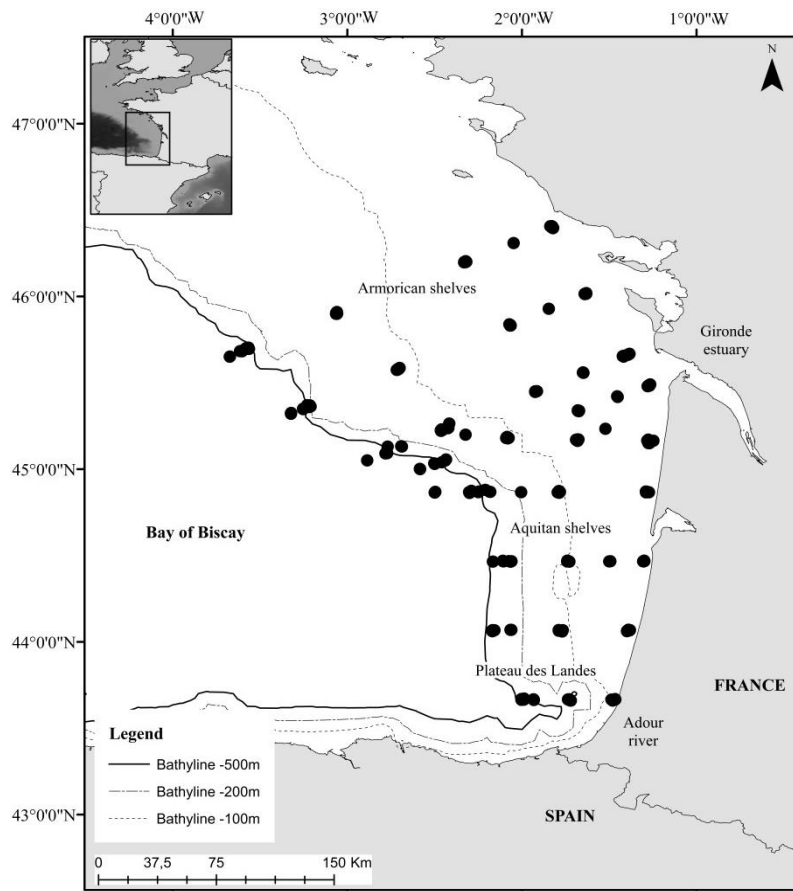
677 **Figure 6:** Non-metric Multi-Dimensional Scaling (NMDS) on adult's copepods dataset in two  
678 panels, above: the plot of the sampling points and below, plot of the copepod taxa (only  
679 keeping the ones having correlation coefficient  $> 0.25$ ). Spatial location of each station was

680 reported by their situation in the Bay of Biscay: coastal (C), continental shelf (Sh) and  
681 continental slope (Sl). The choice of the three temporal groups was based on observations  
682 following Fig. 4A.

683

684 Figure 7: Venn diagram based on a variation partitioning presenting the explained variability  
685 of copepods community with two matrices, H and C. *H* was built with subsurface  
686 temperature, deficit of potential energy and equivalent freshwater height and C with  
687 microphytoplankton (> 20  $\mu\text{m}$ ) biomass at the subsurface (the *chl**a* based-biomass > 20  $\mu\text{m}$ ).  
688 The external square represents the whole variation of the copepod community. Each circle  
689 represents the explanatory tables and values are the part of the variation explained by each  
690 explanatory table. The fraction “Int” is the intersection of the amount of variation explained  
691 by both types of explanatory variables. Statistically significant pure fraction of variation of  
692 copepod community is given in supplemental table 1.

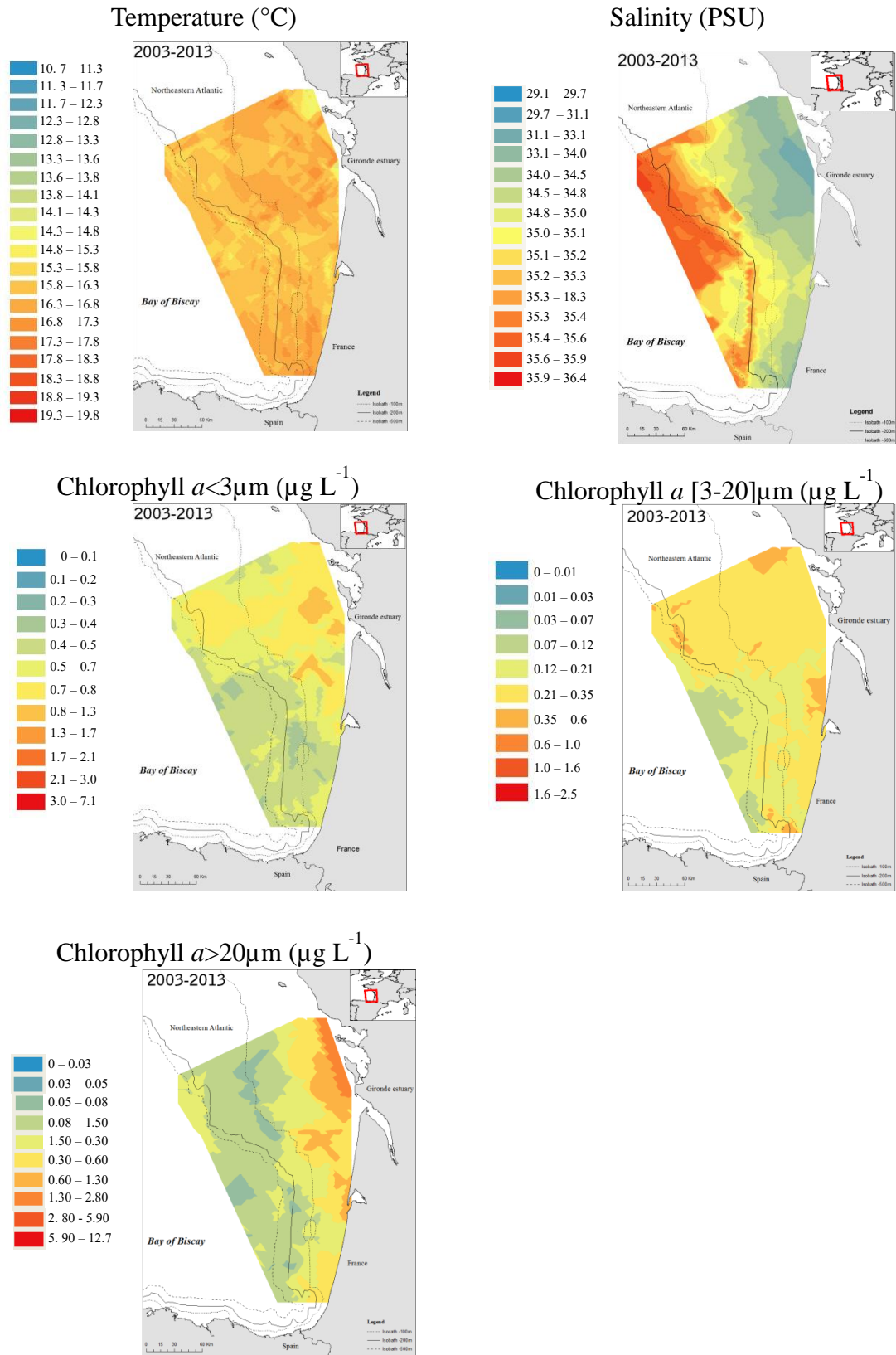
693 **Figure 1**



694

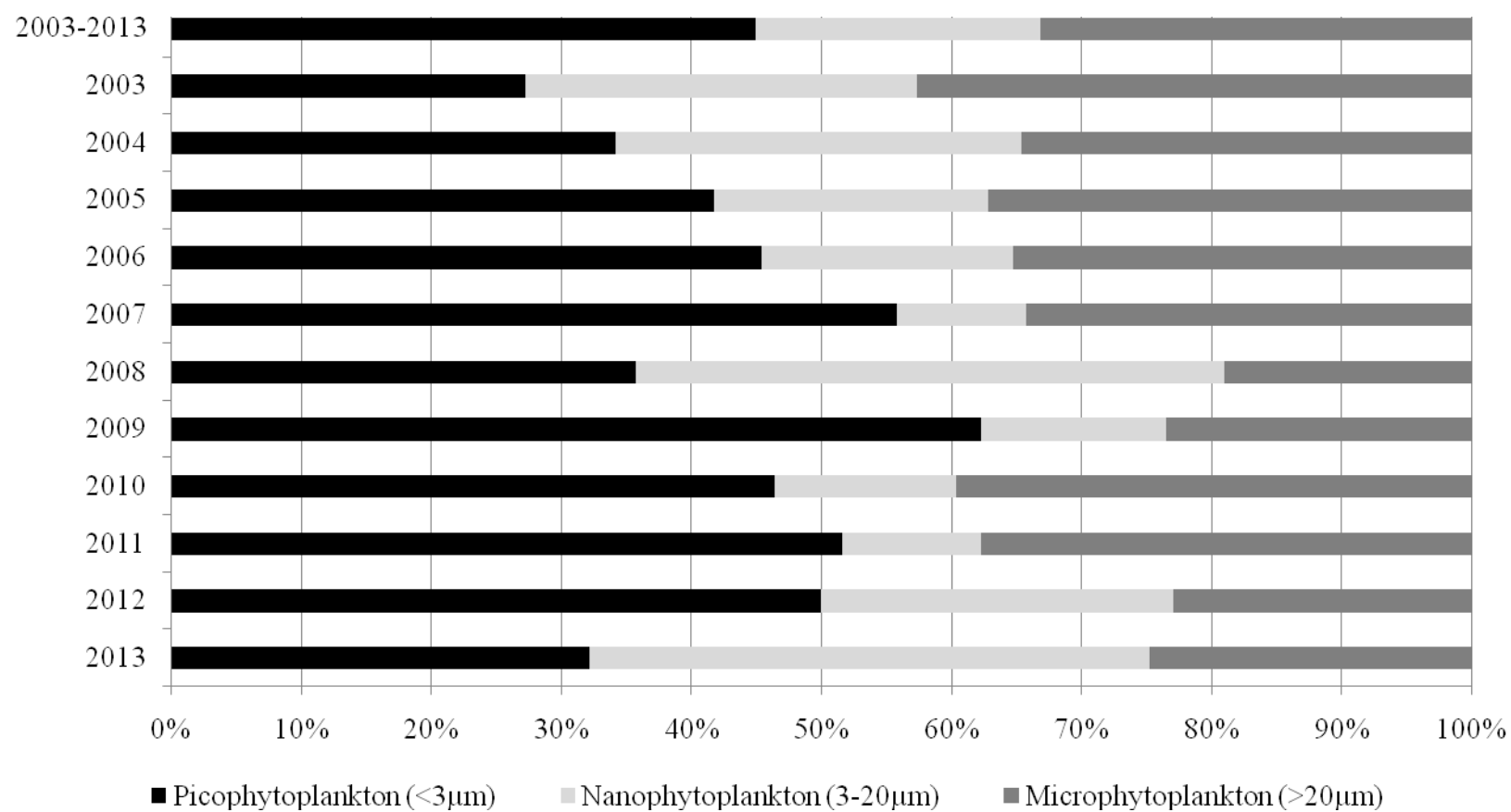
695

696

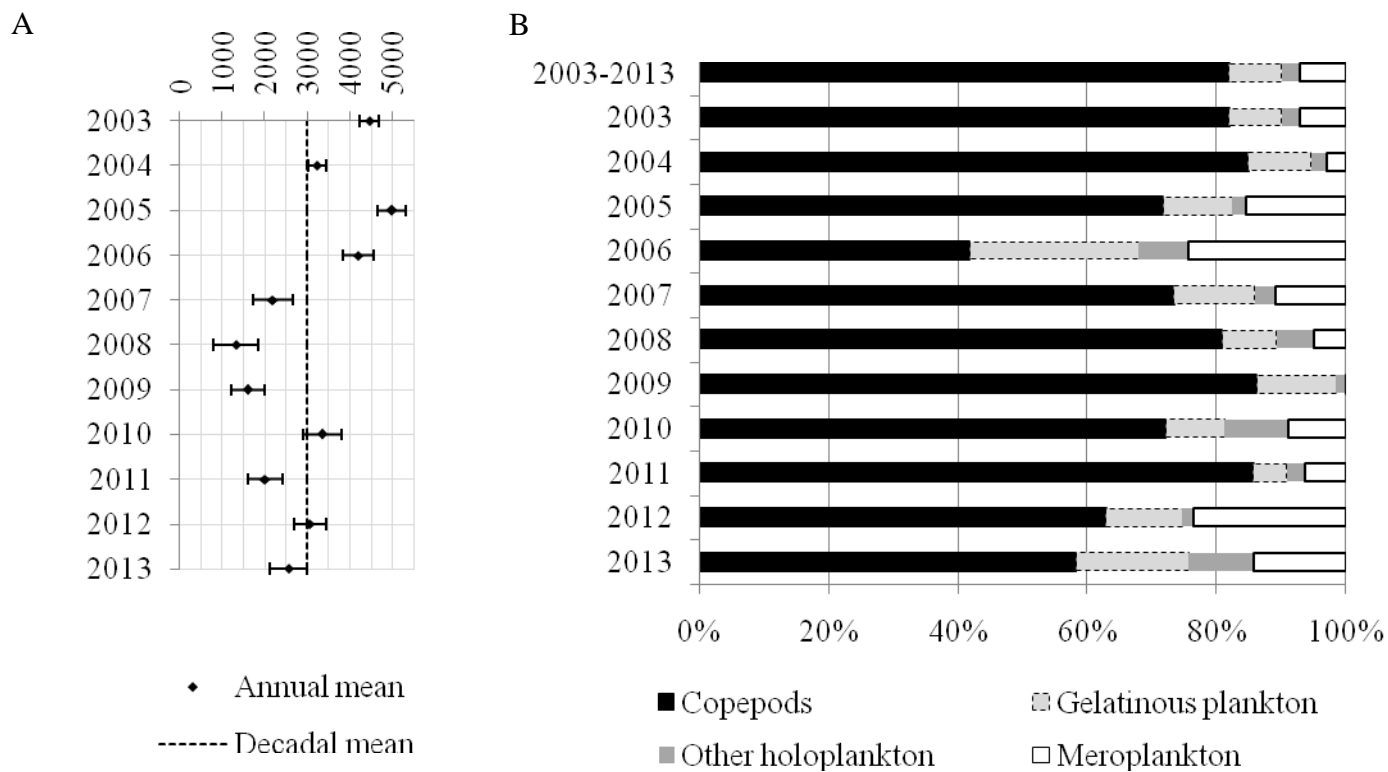


700 **Figure 3**

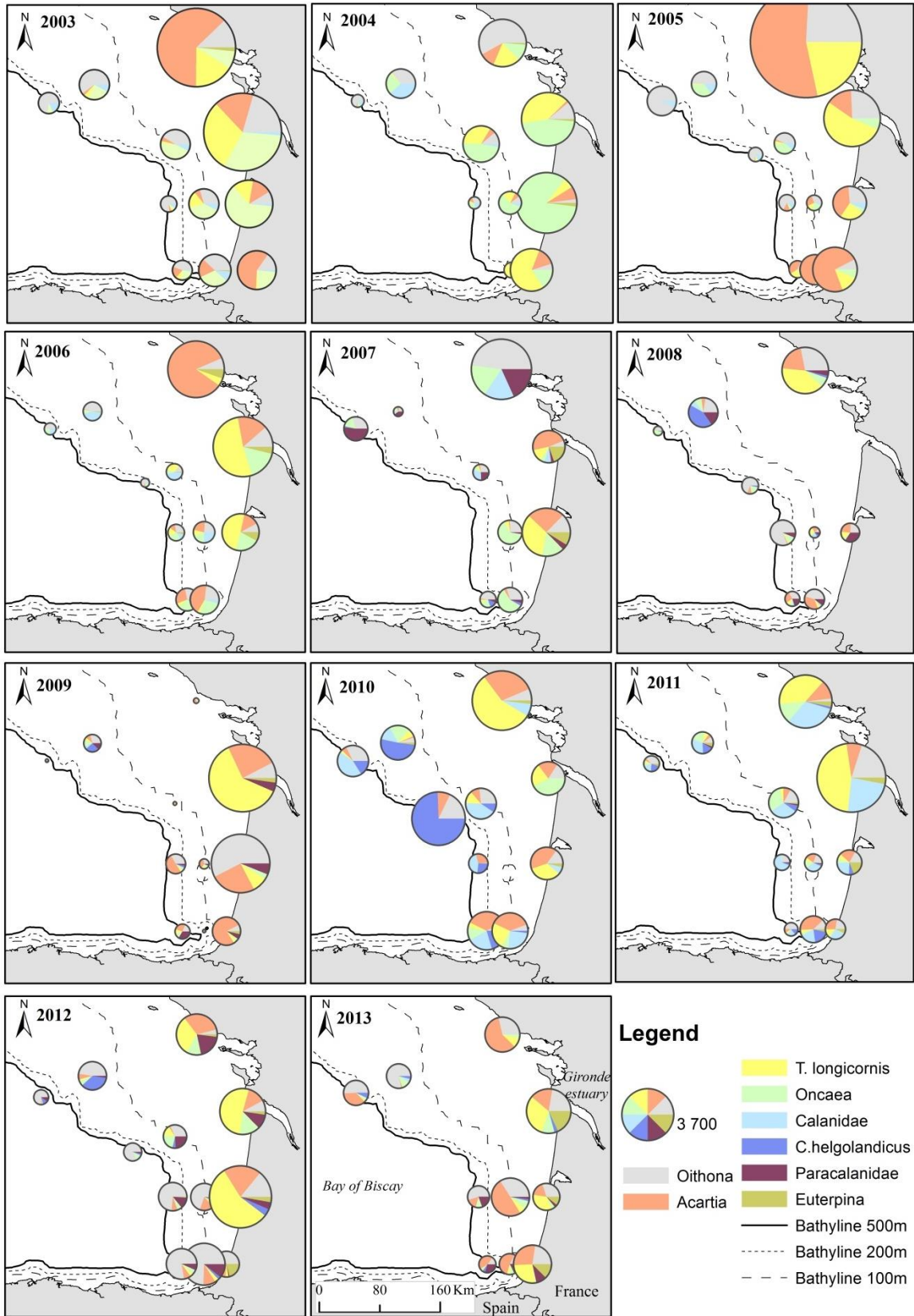
701



702



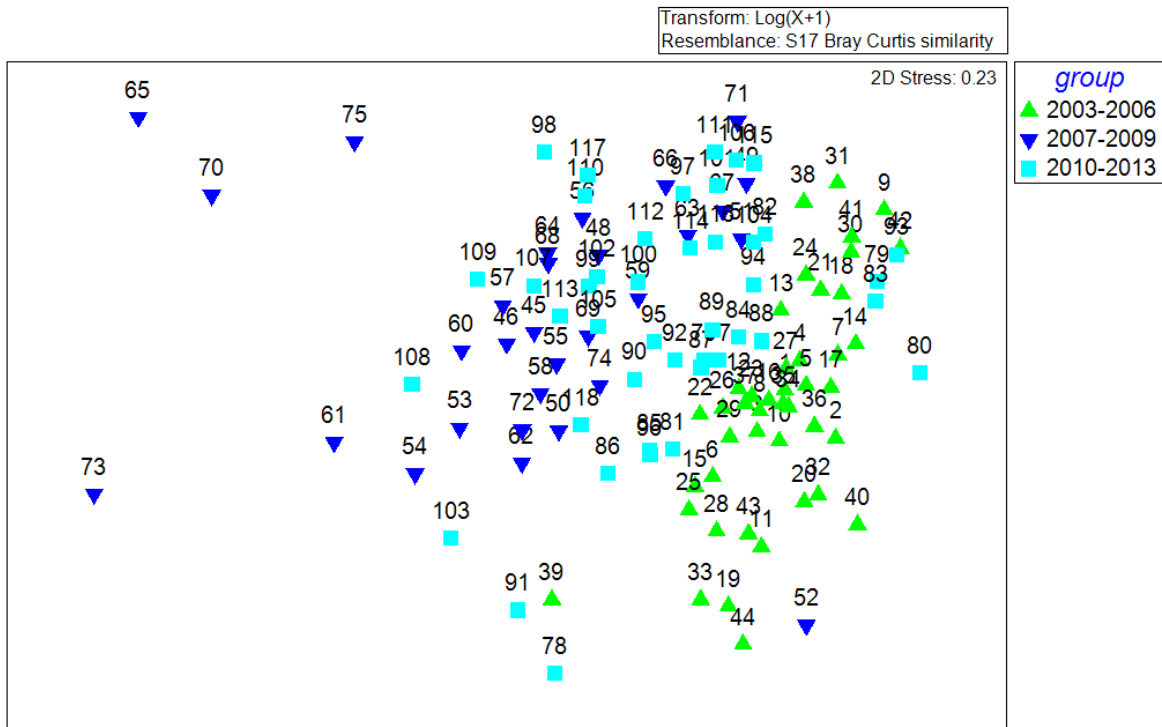
705 **Figure 5**  
706



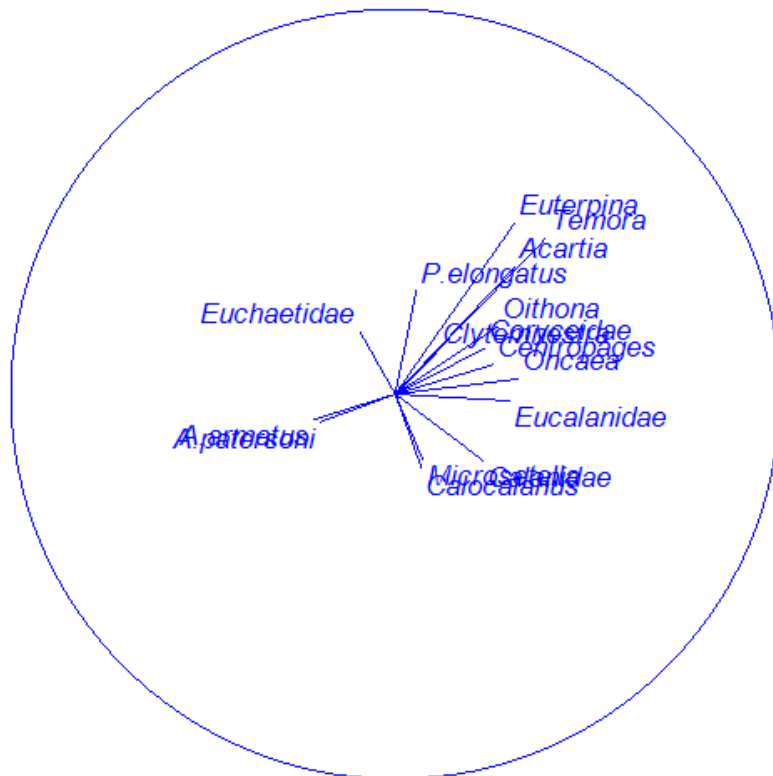
707



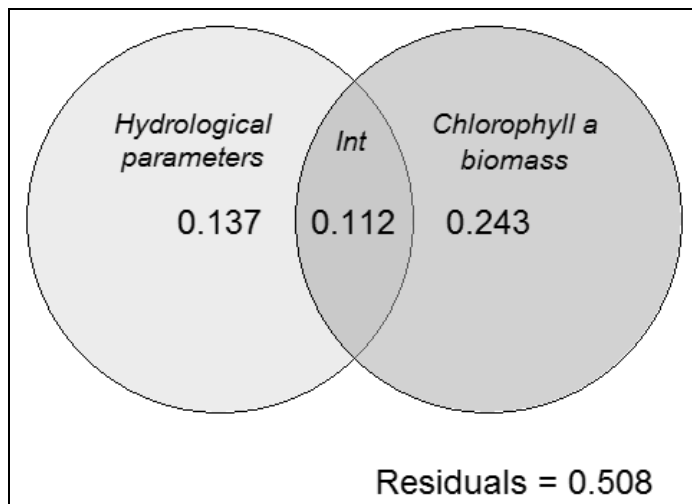
708 **Figure 6**  
 709  
 710  
 711



712  
 713  
 714



715 **Figure 7**  
716  
717



718

719 **Table 1:** Number of stations used in kriging (N.Station.Kriging) and multivariate (N.Station.VarPart) analysis per year start and the end dates of  
 720 the surveys.  
 721

722

723	<b>Year</b>	<b>First Station</b>	<b>Last Station</b>	<b>N.Station.Kriging</b>	<b>N.Station.VarPart</b>
724	2003	30 May	09 June	34	11
725	2004	29 April	10 May	26	10
726	2005	05 May	16 May	30	12
727	2006	02 May	13 May	30	11
728	2007	27 April	08 May	31	10
729	2008	27 April	09 May	31	9
730	2009	26 April	09 May	29	12
731	2010	26 April	09 May	29	10
732	2011	26 April	09 May	28	11
733	2012	27 April	13 May	31	12
734	2013	28 April	16 May	30	10

735

736 **Table 2:** Representative list of taxa and species of mesozooplankton found in the Bay of Biscay with distinction between major groups:  
 737 copepods, gelatinous organisms (G), other holoplankton (H) and meroplankton (M) organisms. For adult copepods, order affiliation is  
 738 represented by Calanoida (Ca), Poecilostomatoida (P), Cyclopoida (Cy) and Harpacticoida (Ha) following by their relative percentage of  
 739 abundance between 2003 and 2013 on copepods community.  
 740

<b>Copepods</b>	<b>Taxonomic level</b>	<b>Order(%)</b>	<b>Other taxonomic groups</b>	<b>Taxonomic level</b>	<b>Group</b>
<i>Acartia</i> spp.	Genus	Ca (19.3)	Appendicularia	Class	G
<i>Oithona</i> spp.	Genus	Cy (18.5)	Siphonophorae	Order	G
<i>Temora longicornis</i>	Species	Ca (17.4)	Indetermined Cnidaria	Phylum	G
Copepodites	Development stage	-(16)	Chaetognata	Phylum	G
<i>Oncaea</i> spp.	Genus	P (10.8)	Salpida	Order	G
Calanidae	Family	Ca (4.5)	Doliolida	Order	G
<i>Calanus helgolandicus</i>	Species	Ca (2.8)	Annelida larvae	Phylum	M
Paracalanidae	Family	Ca (2.2)	Cirripedia	Infra-class	M
<i>Euterpina acutifrons</i>	Genus	H (1.6)	Decapoda	Order	M
<i>Centropages</i> spp.	Genus	Ca (1.5)	Scaphopoda	Class	M
Copepods nauplii	Development stage	-(1.4)	Gastropoda larvae	Class	M

741

742 **Table 2:** continued

<b>Copepods</b>	<b>Taxonomic level</b>	<b>Order(%)</b>	<b>Other taxonomic groups</b>	<b>Taxonomic level</b>	<b>Group</b>
Coryceidae	Family	P (1.3)	Bivalvia larvae	Class	M
Eucalanidae	Family	Ca (1.3)	Enteropneusta	Class	M
<i>Metridia</i> spp.	Genus	Ca (0.4)	Anthozoa larva	Class	M
<i>Pseudocalanus elongatus</i>	Species	Ca (0.5)	Ectoprota	Phylum	M
<i>Microsetella</i> spp.	Genus	H (0.1)	Cyphonauta larvae	Development stage	M
<i>Candacia</i> spp.	Genus	Ca (0.1)	Bryozoa	Phylum	M
<i>Pleuromamma</i> spp.	Genus	Ca (0.1)	Echinodermata larvae	Phylum	M
<i>Calocalanus</i> spp.	Genus	Ca (0.1)	Hydrozoa	Class	M
<i>Clytemnestra</i> spp.	Genus	H (<0.05)	Scyphozoa	Class	M
<i>Aegistus</i> spp.	Genus	H (<0.05)	Ostracoda	Class	H
<i>Aetideus armatus</i>	Species	Ca (<0.05)	Isopoda	Order	H
Euchaetidae	Family	Ca (<0.01)	Mysida	Order	H
Rhincalanidae	Family	Ca (<0.01)	Amphipoda	Order	H
<i>Anomalocera patersoni</i>	Species	Ca (<0.01)	Euphausiacea	Order	H
			Cladocera	Infraorder	H
			Chordata	Phylum	H
			Cumacea	Order	H
			Foraminifera	Phylum	H

743

744 **Table 3:** Results of the similarity percentage (SIMPER) analysis based on spring adult copepods matrix in the Bay of Biscay between 2003 and  
 745 2013.  
 746

<b>Group [2003-2006]</b>		<b>Group [2007-2009]</b>		<b>Group [2010-2013]</b>	
Average similarity: 66.83		Average similarity: 52.32		Average similarity: 59.89	
Genus/Species/Family	Contrib%	Genus/Species/Family	Contrib%	Genus/Species/Family	Contrib%
<i>Oithona</i> spp.	22.4	<i>Oithona</i> spp.	24.37	<i>Oithona</i> spp.	24.02
<i>Oncaea</i> spp.	17.8	<i>Acartia</i> spp.	17.96	<i>Acartia</i> spp.	19.21
<i>Acartia</i> spp.	13.04	<i>Oncaea</i> spp.	17.1	<i>Temora longicornis</i>	13.24
<i>Temora longicornis</i>	12.2	Paracalanidae	15.16	<i>Oncaea</i> spp.	10.96
Eucalanidae	11.94	<i>Temora longicornis</i>	7.77	<i>Calanus helgolandicus</i>	7.95
Calanidae	10.54	Coryceidae	3.76	Calanidae	6.97
<i>Centropages</i> spp.	5.31	<i>Calanus helgolandicus</i>	3.04	Paracalanidae	4.84
		Calanidae	2.9	<i>Euterpina acutifrons</i>	4.11

747  
 748

749 **Table 4:** Results of the dissimilarity percentage (SIMPER) analysis based on spring adult copepods matrix in in the Bay of Biscay between 2003  
 750 and 2013.  
 751  
 752  
 753

Groups [2003-2006] and [2007-2009]		Groups [2003-2006] and [2010-2013]		Groups [2007-2009]and [2010-2013]	
Average dissimilarity: 52.01		Average dissimilarity: 45.51		Average dissimilarity: 46.88	
Genus/Species/Family	Contrib%	Genus/Species/Family	Contrib%	Genus/Species/Family	Contrib%
Eucalanidae	11.04	Eucalanidae	11.29	<i>Temora longicornis</i>	10.09
Paracalanidae	10.49	<i>Calanus helgolandicus</i>	9.44	Calanidae	9.78
<i>Temora longicornis</i>	9.62	Calanidae	8.55	<i>Calanus helgolandicus</i>	9.05
Calanidae	8.59	<i>Temora longicornis</i>	8.46	Paracalanidae	8.79
<i>Acartia</i> spp.	8.2	<i>Acartia</i> spp.	7.85	<i>Acartia</i> spp.	8.39
<i>Oncaea</i> spp.	7.2	<i>Oncaea</i> spp.	7.67	<i>Euterpina acutifrons</i>	7.48
<i>Centropages</i> spp.	6.87	Paracalanidae	7.15	<i>Oncaea</i> spp.	7.38
Coryceidae	6.29	<i>Euterpina acutifrons</i>	7.1	<i>Oithon</i> aspp.	6.31
<i>Oithona</i> spp.	5.77	<i>Centropages</i> spp.	6.92	<i>Centropages</i> spp.	5.99
<i>Euterpina acutifrons</i>	4.98	Coryceidae	6.49	Coryceidae	5.97
<i>Metridia</i> spp.	4.54	<i>Metridia</i> spp.	4.79	<i>Metridia</i> spp.	4.71
<i>Calanus helgolandicus</i>	4.4	<i>Oithona</i> spp.	3.74	<i>Pseudocalanus elongatus</i>	3.46
<i>Candacia armata</i>	2.65	<i>Microsetella</i> spp.	3.06	<i>Candacia armata</i>	3.04

754 **Table 5:** Selection of the most influential variables explaining the most the patterns of copepod community using a forward selection. The eigen  
 755 values sums (a measure of explained variance,  $R^2$ ), “ $F$ ” statistic and p-values were reported.

756  
 757  
 758  
 759

Variables order	Eigenvalues sums	$F$	
Sub-Surface Chla>20µm (Microphytoplankton) Based biomass	0.35	65.28	**
Equivalent fresh water height	0.42	15.47	**
Deficit of potential energy	0.45	7.50	*
Sub-surface temperature	0.49	8.84	**

Codes:0 ‘\*\*\*’;0.001 ‘\*\*’;0.01 ‘\*’

760







763 **List of supplemental figures**

764 **Supplemental figure S1:** Annual interpolated maps of results of the annual spatial  
765 interpolation of sub-surface temperature measures ( $^{\circ}\text{C}$ ), performed for each year between  
766 2003 and 2013 in the southern Bay of Biscay. Thanks to a non-parametric multiple pairwise  
767 comparison of mean ranks applied for all years, significant differences of sub-surface  
768 temperature according to year are indicated by letters.

769 **Supplemental figure S2:** Annual interpolated maps of results of the spatial interpolation of  
770 sub-surface salinity (PSU<sub>psu</sub>) performed for each year between 2003 and 2013, in the  
771 southern Bay of Biscay.

772 **Supplemental figure S3:** Annual interpolated maps of results of the spatial interpolation of  
773 sub-surface picophytoplankton ( $\text{chl}a < 3\mu\text{m}$ ) biomass ( $\mu\text{g}\cdot\text{L}^{-1}$ ) performed for each year  
774 between 2003 and 2013, in the southern Bay of Biscay. Thanks to a non-parametric multiple  
775 pairwise comparison of mean ranks applied for all years, significant differences of sub-surface  
776 picophytoplankton biomass according to year are indicated by letters.

777 **Supplemental figure S4:** Annual interpolated maps of results of the spatial interpolation of  
778 sub-surface nanophytoplankton ( $[3-20]\mu\text{m}$ ) biomass ( $\mu\text{g}\cdot\text{L}^{-1}$ ) performed for each year  
779 between 2003 and 2013, in the southern Bay of Biscay. Thanks to a non-parametric multiple  
780 pairwise comparison of mean ranks applied for all years, significant differences of sub-surface  
781 nanophytoplankton biomass according to year are indicated by letters.

782 **Supplemental figure S5:** Annual interpolated maps of Results of the spatial interpolation of  
783 sub-surface microphytoplankton ( $\text{chl}a > 20\mu\text{m}$ ) biomass ( $\mu\text{g}\cdot\text{L}^{-1}$ ) performed for each year  
784 between 2003 and 2013, in the southern Bay of Biscay. Thanks to a non-parametric multiple  
785 pairwise comparison of mean ranks applied for all years, significant differences of sub-surface  
786 microphytoplankton biomass according to year are indicated by letters.

787

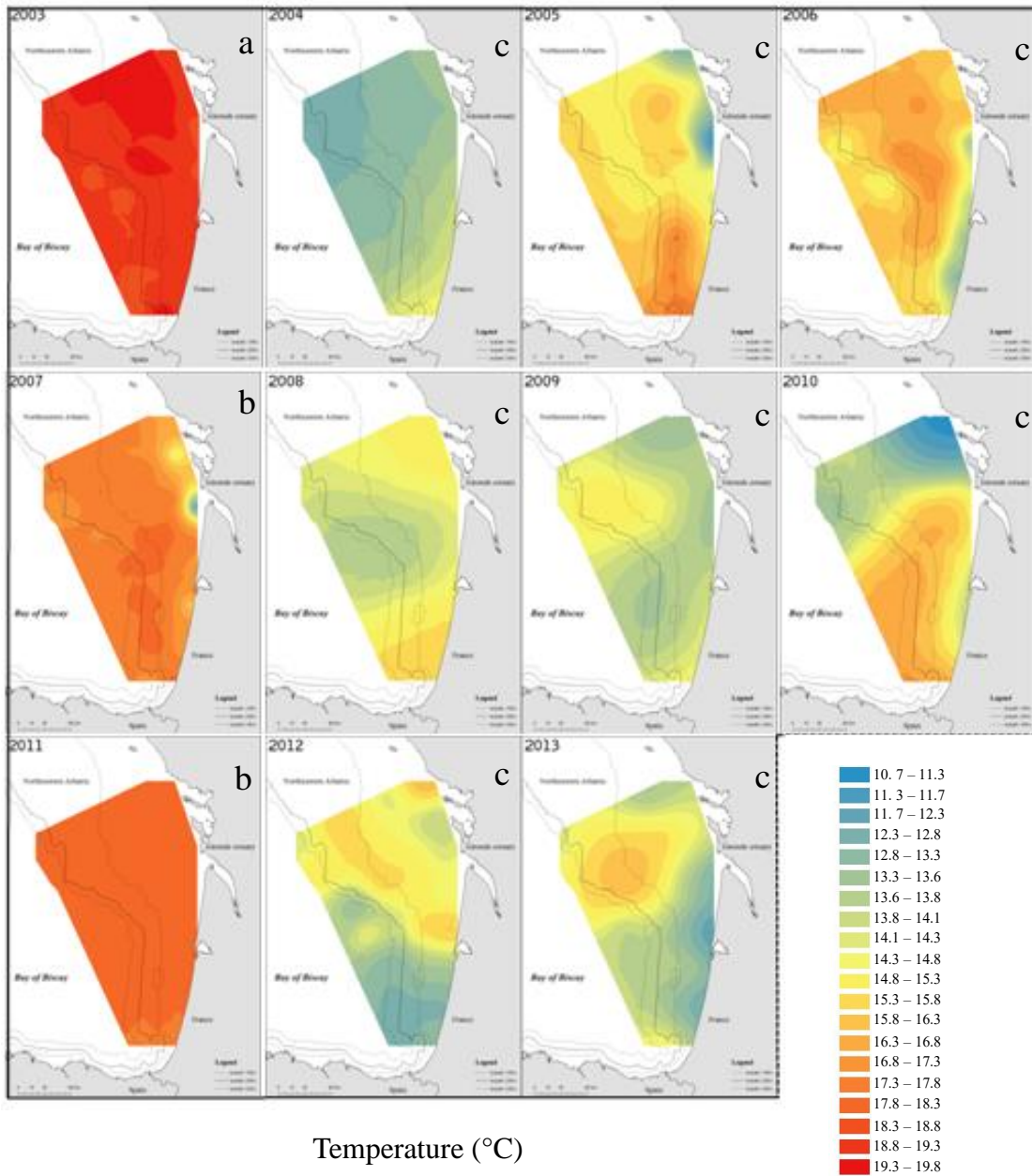
788 **Supplemental figure S6:** Spatial distribution of abundance (ind.m<sup>-3</sup>) of copepods nauplii,  
789 copepodites and Harpacticoida, Poecilostomatoida, Cyclopoida, Calanoida (orders) between  
790 2003 and 2013 in the southern Bay of Biscay. The size of the pies is proportional to the total  
791 abundance of from each station throughout the decade. Significant differences in abundance  
792 according to year are indicated by letters.

793 **Supplemental figure 1:**

794

795

796



797

798 **Supplemental figure 2:**

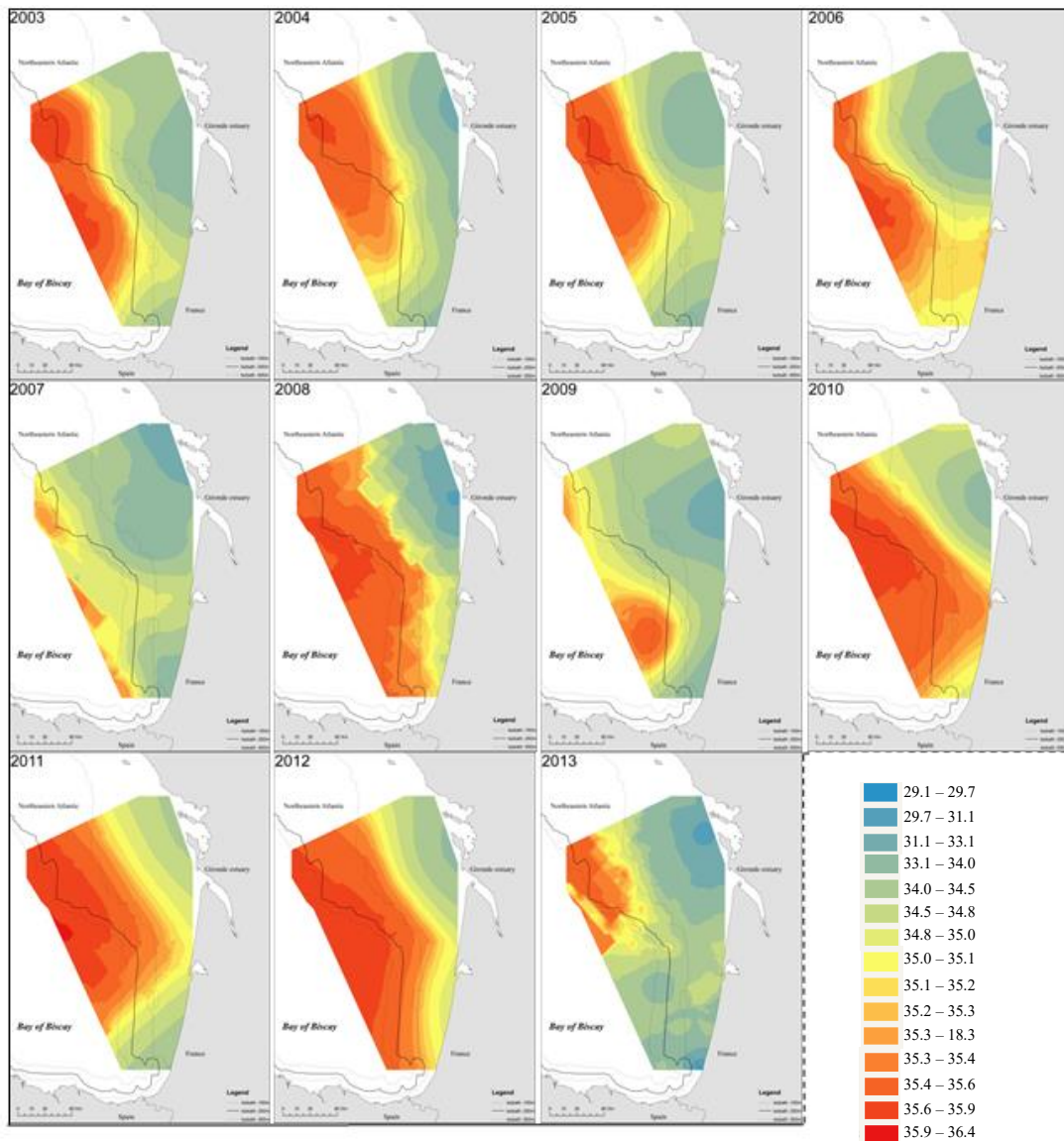
799

800

801

802

803



Salinity (PSU)

804

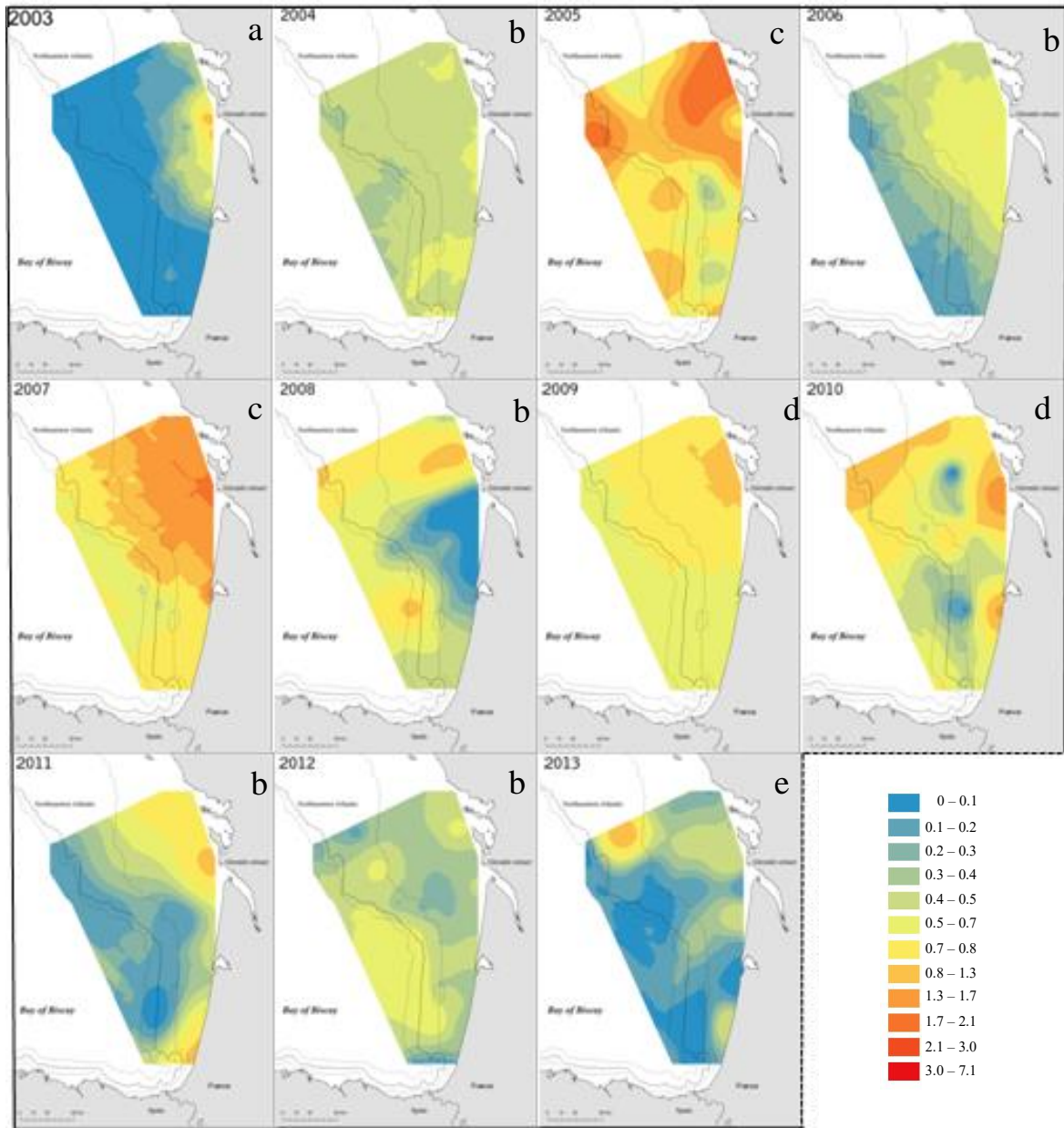
805 **Supplemental figure 3:**

806

807

808

809



810

811

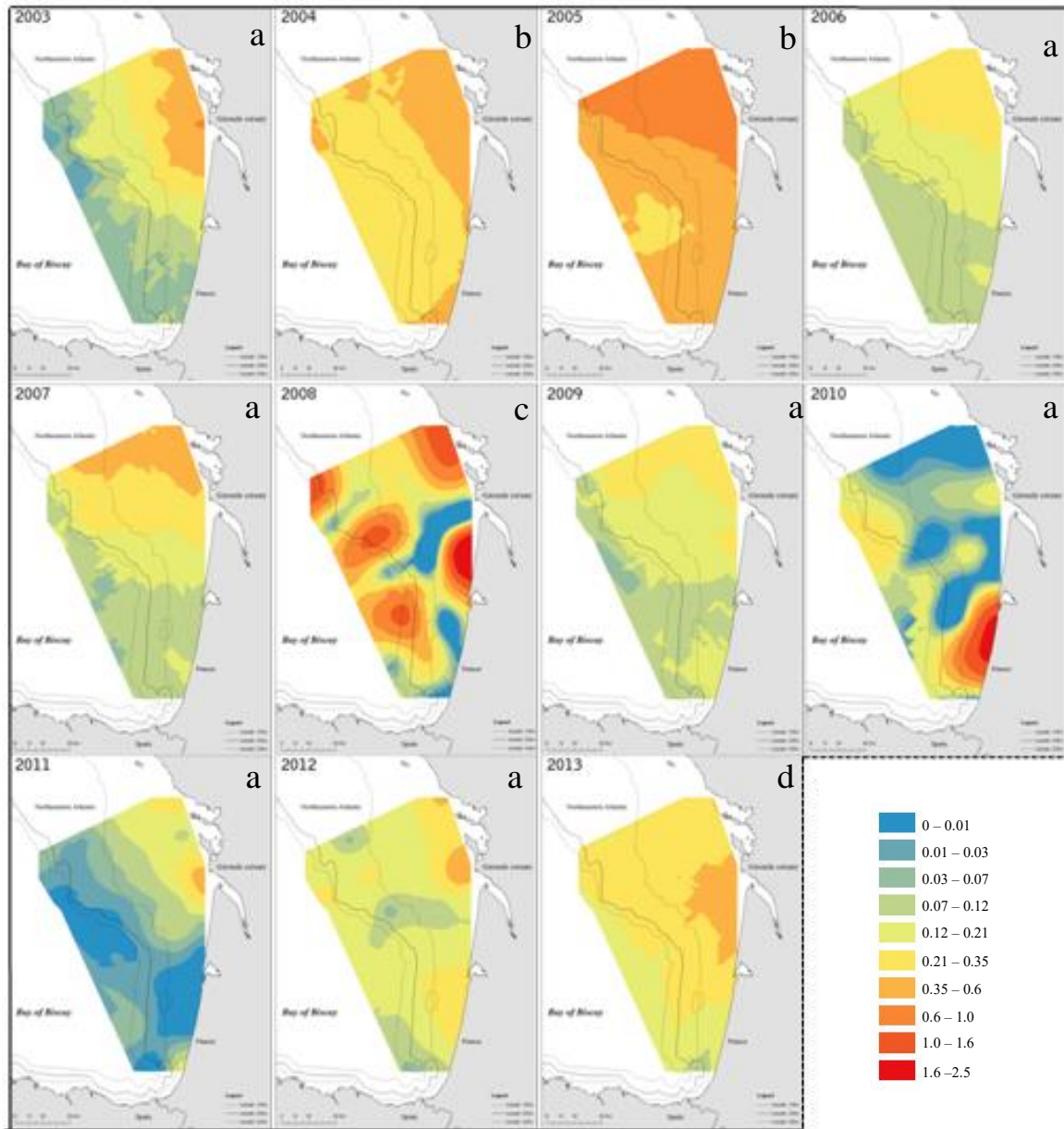
812 **Supplemental figure 4:**

813

814

815

816



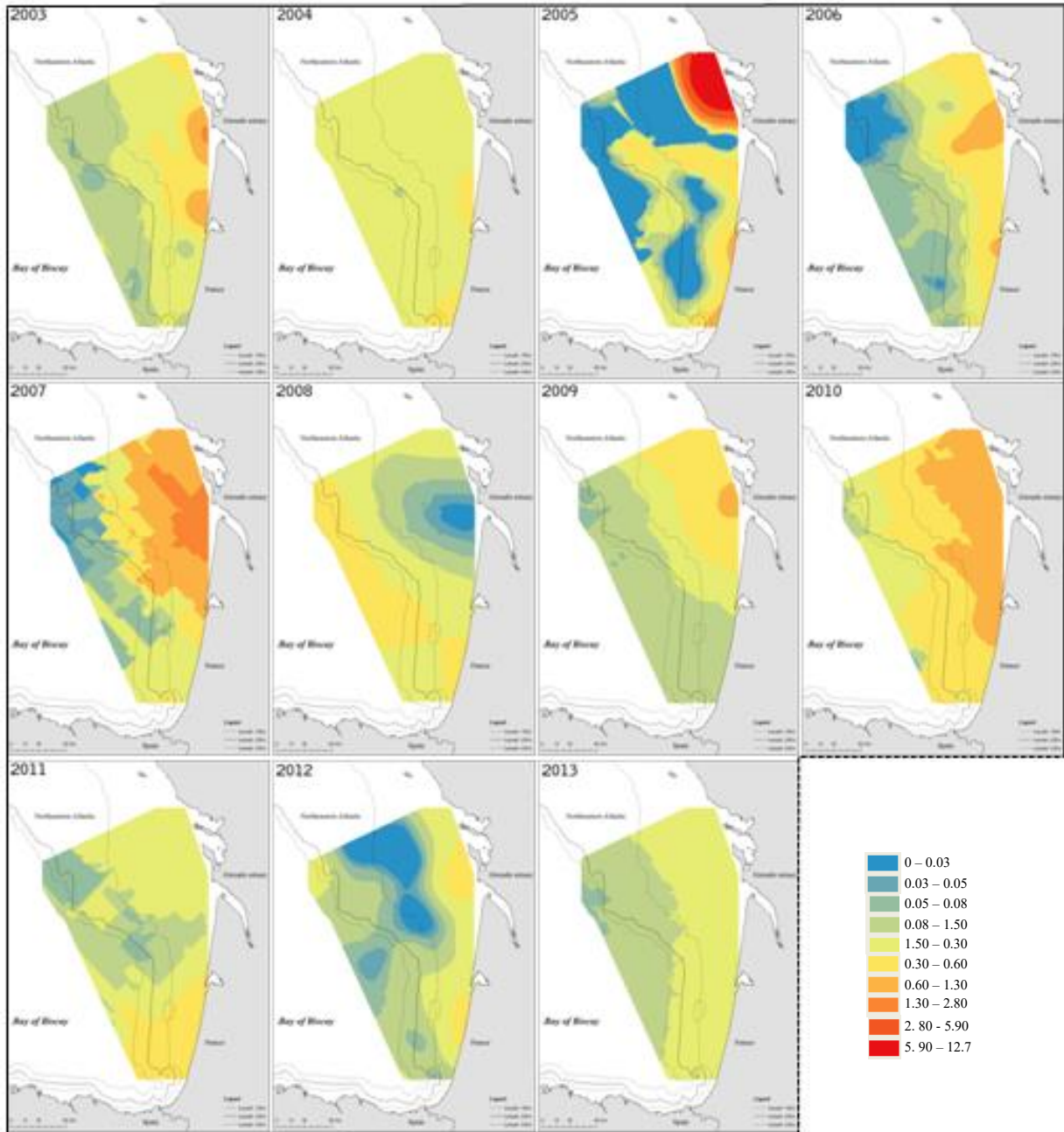
Chlorophyll *a* [3-20]µm ( $\mu\text{g L}^{-1}$ )



817 **Supplemental figure 5:**

818

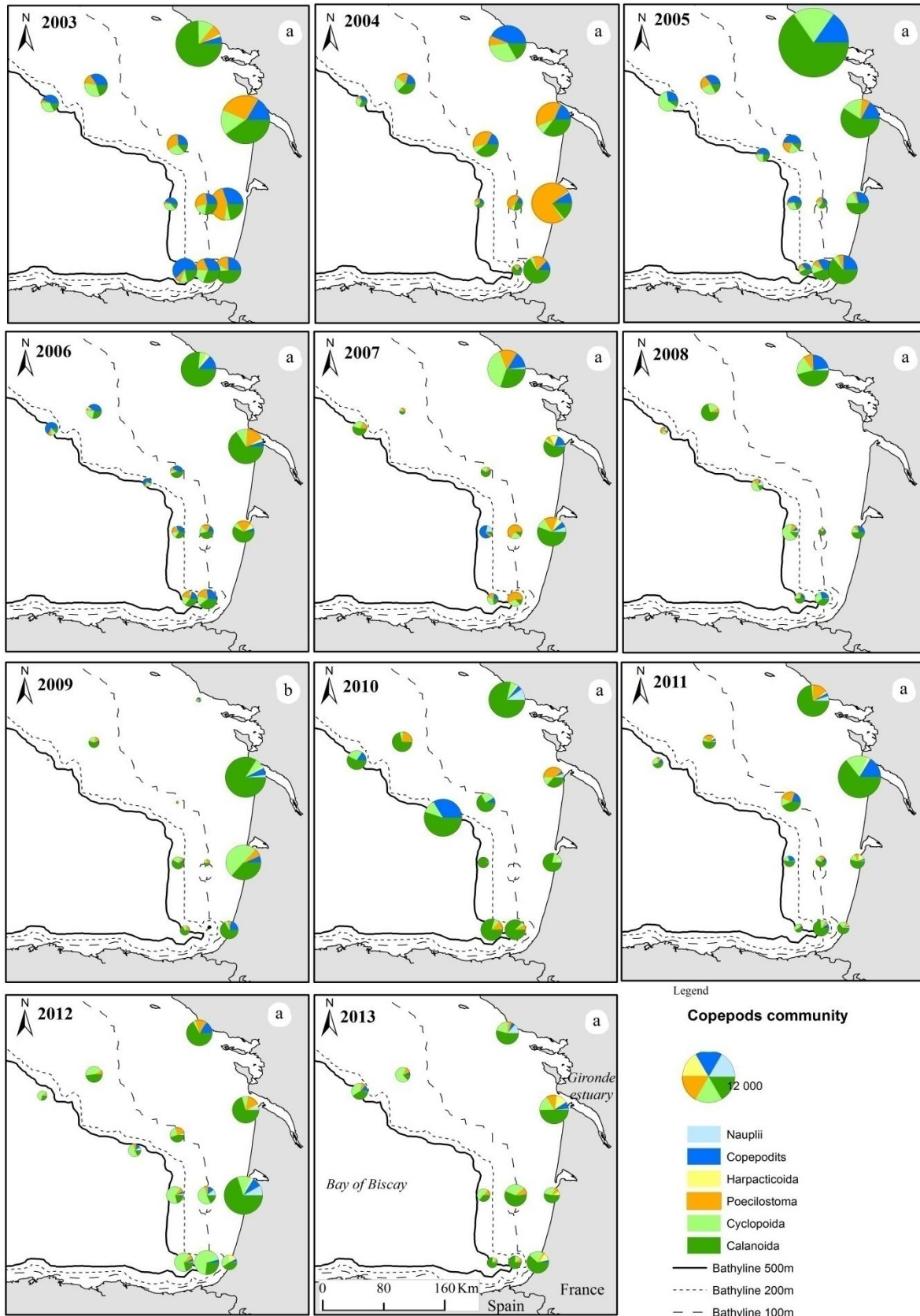
819



Chlorophyll *a*<sub>>20 $\mu\text{m}$</sub>  ( $\mu\text{g L}^{-1}$ )

820 **Supplemental figure 6:**

821



822

823

824 **List of supplemental figure :**

825 **Supplemental table 1:** Identification of copepod community drivers by variation partitioning  
 826 analysis based on ordination analyses. Matrix H contained environmental variables (sub-  
 827 surface temperature values, deficit of potential energy and equivalent freshwater height),  
 828 matrix C contained the chlorophyll *a* >20 µm biomass (microphytoplankton biomass).  
 829 Multivariate analysis, covariables, component of variation, eigenvalues and statistical p-  
 830 values are reported. Explanatory matrix / component of variation; H/h – hydrological  
 831 parameters, C/c – chlorophyll *a* based biomass.

832  
 833  
 834

Analysis	Constraining variable	Covariate	Component of the variation	Eigenvalues sums	<i>p-value</i>
ACP	-	-	-		
RDA	H		h + hc	0.24	***
RDA	C		c + hc	0.35	***
RDA	H+C		h + c + hc	0.49	***
RDAp	H	C	h	0.13	***
RDAp	C	H	c	0.24	**

Codes for p-values: 0 '\*\*\*';0.001 '\*\*';0.01 '\*'

835

836